

# InternLM-XComposer: A Vision-Language Large Model for Advanced Text-image Comprehension and Composition

Pan Zhang<sup>\*1</sup>, Xiaoyi Dong<sup>\*1</sup>, Bin Wang<sup>1</sup>, Yuhang Cao<sup>1</sup>, Chao Xu<sup>1</sup>, Linke Ouyang<sup>1</sup>, Zhiyuan Zhao<sup>1</sup>, Haodong Duan<sup>1</sup>, Songyang Zhang<sup>1</sup>, Shuangrui Ding<sup>1</sup>, Wenwei Zhang<sup>1</sup>, Hang Yan<sup>1</sup>, Xinyue Zhang<sup>1</sup>, Wei Li<sup>1</sup>, Jingwen Li<sup>1</sup>, Kai Chen<sup>1</sup>, Conghui He<sup>1</sup>, Xingcheng Zhang<sup>1</sup>, Yu Qiao<sup>1</sup>, Dahua Lin<sup>1</sup>, Jiaqi Wang<sup>1,✉</sup>

<sup>1</sup>Shanghai Artificial Intelligence Laboratory

internlm@pjlab.org.cn

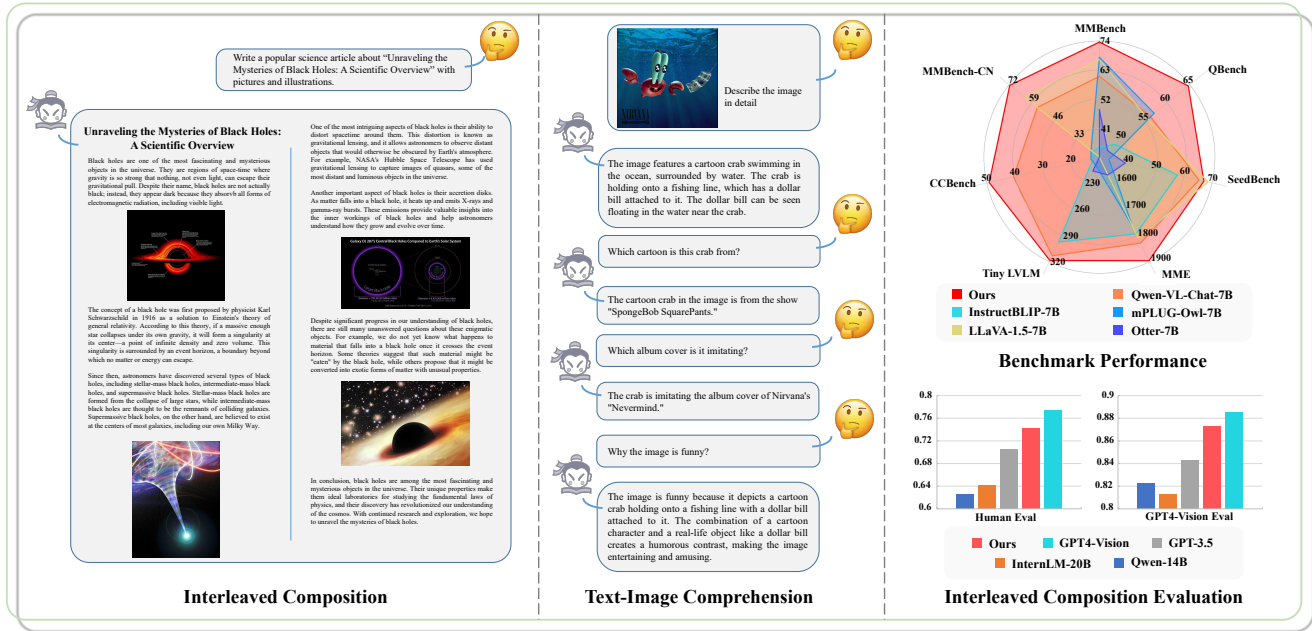


Figure 1. The InternLM-XComposer shows excellent interleaved composition and text-image comprehension ability, leading to strong performance on various multi-modal benchmarks. For the Interleaved Composition Evaluation by both Human and GPT4-Vision (GPT4-V), our model shows competitive performance to GPT4-Vision and GPT3.5.

## Abstract

We propose *InternLM-XComposer*, a vision-language large model that enables advanced image-text comprehension and composition. The innovative nature of our model is highlighted by three appealing properties: 1) **Interleaved Text-Image Composition**: *InternLM-XComposer* can effortlessly generate coherent and contextual articles that seamlessly integrate images, providing a more engaging and immersive reading experience. Simply provide a writing instruction, and our system will generate the corresponding manuscript. It can intelligently identify the areas in the text where images would enhance the content and automatically insert the most appropriate vi-

sual candidates. 2) **Comprehension with Rich Multilingual Knowledge**: The text-image comprehension is empowered by training on an extensive multi-modal multilingual database with carefully crafted strategies, resulting in a deep understanding of visual content. 3) **State-of-the-art Performance**: Our model consistently achieves state-of-the-art results across various mainstream benchmarks for vision-language foundational models, including MME Benchmark, MMBench, MMBench-CN, SeedBench, CCBench (Chinese Cultural Benchmark), QBench and Tiny L2LM. Owing to the absence of established metrics for quantitatively assessing text-image composition, we have devised a robust evaluation procedure that comprises both human and GPT4-Vision (GPT4-V) to ensure reliability. Notably, our *InternLM-XComposer* achieves competitive text-image composition scores compared to pub-

\* indicates equal contribution.

lic solutions, including GPT4-V and GPT3.5. Collectively, InternLM-XComposer seamlessly blends advanced text-image comprehension and composition, revolutionizing vision-language interaction and offering new insights and opportunities. The InternLM-XComposer model series are publicly available at <https://github.com/InternLM/InternLM-XComposer>.

## 1. Introduction

Over the past year, impressive progress has been made in developing large language models (LLMs) [5, 7, 15, 16, 24, 60, 61, 66, 69, 84–86]. These state-of-the-art models, including ChatGPT [60], GPT4 [61], and PaLM 2 [16], have shown an unprecedented ability to follow human instructions and solve open-ended tasks. Inspired by the success of PaLM-E [23] and BLIP2 [42], there is a promising approach to extending language models for vision-language tasks by leveraging vision features as extra inputs of LLMs. The community has developed several vision-language large models (VLLMs), such as MiniGPT-4 [104], LLaVA [50], and InstructBLIP [18], based on open-source LLMs like LLaMA [85], GLM [24], and InternLM [84]. However, these VLLMs focus on pure text outputs, missing the opportunity to equip generated text with richer information through auxiliary multimedia content like images.

In this work, we propose InternLM-XComposer, which is a vision-language large model that enables advanced text-image comprehension and composition ability.

1) **Interleaved Text-Image Composition.** InternLM-XComposer excels in generating long-form content that is interleaved with contextually relevant images, providing more engaging and immersive vision-language interactions. In its operational flow, the framework first crafts articles following human-provided instructions. Subsequently, it autonomously pinpoints optimal locations within the text for image placement and furnishes corresponding suitable image descriptions. In accordance with the generated descriptions, instead of relying on text-to-image generation models [6, 70–73], we opt to source aligned images from a large-scale web-crawled image database for realistic quality and contextual alignment. Moreover, it also provides flexibility by allowing users to customize an image repository.

Compared to a baseline approach that relies solely on CLIP [67, 92] for image retrieval, XComposer offers a more reliable solution for choosing the most appropriate image. Initially, we select potential image candidates from our database using CLIP. Then, InternLM-XComposer leverages its comprehension capabilities to identify the image that optimally complements the content.

2) **Comprehension with Rich Multilingual Knowledge.** LLM demonstrates remarkable ability in handling open-world tasks, a capability attributed to its extensive

training data, e.g., 2T text tokens used in LLaMA2 [86]. This vast dataset inherently encapsulates a broad spectrum of semantic knowledge across diverse domains. In contrast, current vision-language datasets [8, 62, 75, 78] are limited in both volume and diversity compared to the LLM database. This results in insufficient coverage of vision-language concepts due to the long-tailed data distribution [17, 54, 59] in the real world. To tackle this limitation, we employ two practical solutions: First, to extend the knowledge of VLLMs with widespread concepts, a multilingual vision-language dataset comprising over 11 million semantic concepts is collected from public websites. We further gather open-sourced vision-language datasets to organize our high-quality training data. Second, we carefully crave the pretraining and finetuning strategies in our training pipeline, where we adopt the mixed training data of pure text and image-text data, primarily in English and Chinese, to keep the initial capabilities of LLMs. Consequently, InternLM-XComposer demonstrates a remarkable proficiency in comprehending image content and responding with extensive multilingual knowledge. InternLM-XComposer stands out for its unique ability to compose long-form articles that incorporate contextually relevant images. This process involves creating high-quality written content, identifying appropriate positions for inserted images, and selecting the most suitable images that consider the complex context of interleaved text and images.

The proposed InternLM-XComposer exhibits superior capabilities in both text-image comprehension and composition, as evidenced by its strong performance in quantitative benchmarks and compelling qualitative demonstrations. It consistently achieves **state-of-the-art** performance across various leading benchmarks for vision-language large models, encompassing MME Benchmark [26, 95], MMBench [52], Seed-Bench [40], QBench [90], Tiny LLaVA [77] in English, and MMBench-CN [52], CCBench (Chinese Cultural Benchmark) [52] for evaluations in Chinese. Furthermore, in response to the absence of established metrics for quantitatively assessing text-image composition, we set up an evaluation procedure for interleaved text-image articles. This procedure takes into account the quality of both the written content and the accompanying illustrated images, which harnesses both human assessment and GPT4-Vision (GPT4-V) scoring to enhance robustness and reliability. The evaluation outcomes, spanning assessments by both human and GPT4-V, consistently demonstrate the competitive performance of InternLM-XComposer in interleaved text-image composition compared to public solutions, including GPT3.5 and GPT4-V.

## 2. Related Works

**Large Language Models (LLMs).** In recent years, the development of large language models has accelerated. Ini-

tially, encoder-decoder models such as BERT [21] and T5 [69], as well as decoder-only models like GPT [68], leveraged the Transformer architecture [87] to achieve remarkable results. GPT3 [7], employing prompt and in-context learning strategies along with larger models and data, has significantly performed in few-shot and zero-shot tasks. As a result, using decoder-only structures with autoregressive training has gained popularity among researchers. Google’s PaLM [16] further expands the model parameter size and data volume. To enhance the conversational experience, models like InstructGPT [63] and ChatGPT [60] integrate instruction-tuning and reinforcement learning from human feedback (RLHF). The open-sourcing of LLaMA [85] model has inspired research on LLMs, e.g., Alpaca [83], Vicuna [15], GLM [24, 97], Qwen [66], LLaMA2 [86], Baichuan2 [5], InternLM [84], Falcon [64], and Mistral [36].

**Vision Large Language Models (VLLMs).** Visual language learning has emerged as a research hotspot. CLIP [67] and its following works [43, 45, 51, 99] aligns image and text features through contrastive learning objectives on large-scale image-text pairs, outperforming supervised learning on ImageNet [20] and exhibiting strong generalization capabilities in various downstream tasks. However, these models show limited capabilities for tasks requiring higher-level understanding, such as visual question answering. Benefiting from existing large language model [15, 69, 85] and visual encoder [25, 43], the vision large language models (VLLMs) [11, 13, 14, 23] achieve fine-grained alignment between the visual information and the LLMs, show superb performance in diverse tasks. To achieve the modality alignment, a series of studies [1, 3, 9, 10, 41, 50, 65, 88, 94, 101, 103] have explored the impact of the quality, diversity, and specificity of the fine-tuning data and the learnable parameters. For example, MiniGPT4 [104] adopts a simple FC layer with a small amount of caption data. InstructBLIP [18] fine-tunes the Q-Former [43] on diverse image-text tasks. LLaVA [50] fine-tunes the LLM with GPT-4 generated high-quality instruction tuning data. Qwen-VL [4] and CogVLM [89] fine-tune on high-resolution images with multi-task training. Moreover, some recent works [22, 28, 82, 96] integrate the image generation task with VLLMs to generate text-aligned images. InternLM-XComposer stands out for its unique ability to compose long-form articles that incorporate contextually relevant images. This process involves creating high-quality written content, identifying appropriate positions for inserted images, and selecting the most suitable visual content that considers the interleaved vision-language context.

**Image-text Retrieval Models.** Image-text retrieval, a pivotal area in multimodal modeling, has seen substantial advancements recently. CLIP [67] and its following

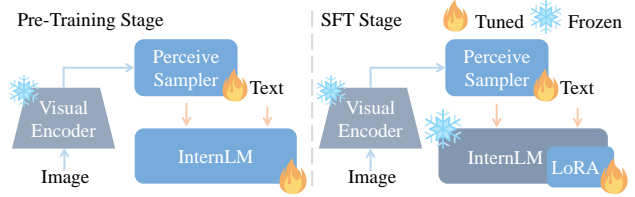


Figure 2. The architecture and training regimen of the InternLM-XComposer. The Pre-training stage aligns the visual and language knowledge and the SFT stage excites different model capabilities.

works [33, 35, 37, 43, 93, 100] utilize contrastive learning on a large corpus of image-text pairs, excels in image-text matching, enabling efficient retrieval in both image-to-text and text-to-image modalities. However, the capabilities of current models are primarily confined to matching images with aligned descriptions, which has a significant gap between our image-text article composition task, which focuses on selecting a suitable image based on a complex context containing interleaved images and long text.

### 3. Method

#### 3.1. Model Architecture

As depicted in Figure 2, the proposed InternLM-XComposer contains three integral components: a visual encoder, a perceive sampler, and a large language model.

**Visual Encoder.** The visual encoder in InternLM-XComposer employs EVA-CLIP [25], an refined variant of the standard CLIP [92], enhanced with mask image modeling capabilities, to proficiently capture the visual nuances of the input image. Within this module, images are resized to a consistent dimension of  $224 \times 224$  and subsequently dissected into patches with a stride of 14. These patches serve as input tokens and enable the self-attention mechanisms within the transformer block, facilitating the extraction of detailed image embeddings.

**Perceive Sampler.** The perceive sampler within the InternLM-XComposer operates as an attentive pooling mechanism designed to condense the initial set of 257 image embeddings down to 64 refined embeddings. These optimized embeddings are subsequently aligned to be compatible with the knowledge structures understood by the large language model. Following BLIP2 [42], we leverage BERT<sub>base</sub> [21] equipped with cross-attention layers, serving as the perceive sampler in our framework.

**Large Language Model.** The InternLM-XComposer is anchored on InternLM [84] as its foundational large language model. Notably, InternLM stands as a potent language model equipped with multilingual capabilities, proficient in both English and Chinese. In our framework, we employ the publicly available InternLM-Chat-7B to serve as the large language model.

Language	Type	Dataset	Images	Text
English	Pure Text	WanJuan [30]	-	5B
	Paired	CC 3M [78]	3M	37M
	Paired	SBU-Caption [62])	1M	18M
	Paired	LAION400M [75]	509M	10B
	Paired	CC 12M [8]	9M	250M
	Paired	In-house Concept data	2M	321M
	Interleaved	Multimodal C4 [105]	332M	40B
Chinese	Pure Text	WanJuan [30]	-	5B
	Paired	TaiSu [53]	44M	865M
	Paired	WuKong [29]	31M	545M
	Paired	LAION-CN [74]	80M	2B
	Paired	In-house Concept data	9M	704M
	Interleaved	WanJuan [30]	85M	13B
Total			1.1B	77.7B

Table 1. Details of InternLM-XComposer pre-training data. LAION-CN represents the Chinese language subset extracted from the larger LAION-5B corpus. This subset is further cleaned utilizing the Chinese CLIP [92]. The volume of text data is counted in terms of the number of tokens. The In-house Concept data is collected from public websites, including over 11 million vision-language concepts from public websites.

Task	Dataset
<i>Multi-task training</i>	
Caption	COCO [12], SUB [12], TextCaps [79]
VQA	VQAv2 [2], GQA [34], OK-VQA [57], IConQA [56] Text-VQA [80], SQA [55], VSR [47], OCR-VQA [58], VIGC [88]
IQG	VQAv2 [2], OK-VQA [57], A-OKVQA [76]
Conversation	Visual Dialog [19], LLaVA-150k [50]
<i>Instruction tuning</i>	
Compositon	In-house data (Refer to Sec.3.3)
Conversation	LLaVA-150k [50], Alpaca-en&zh [83] ShareGPT-en&zh [15], Oasst-en&zh [38], LRV [48]

Table 2. Datasets used for Supervised Fine-Tuning.

### 3.2. Training

As shown in Figure 2, the training process of InternLM-XComposer is split into Pre-training Stage and Supervied Fine-tuning (SFT) Stage. The pre-training stage utilizing vast amounts of data for foundation model training, aligning the knowledge between the visual information and language. Based on the pre-training model, the SFT stage involves a multi-task training step and a following instruction tuning step to excite different model capabilities.

**Pre-training.** The pre-training phase incorporates large-scale image-text pairs along with interleaved image-text data to pre-train the foundational vision-language model. This data comprises multi-modal content in both English and Chinese. As shown in Table 1, in addition to public datasets, to enhance the ability of MLLMs to comprehend extensive visual concepts, we collect large-scale **In-**

**house Concept data**<sup>1</sup> from various public websites, including more than 11 million visual concepts and corresponding details explanations. Please refer to supplementary materials for more information. Moreover, to preserve the capabilities of the initial large language model, the partial textual data [30] utilized for InternLM’s pre-training is also employed in the pre-training phase of InternLM-XComposer. The multi-modal pre-training process employs 1.1 billion images alongside 77.7 billion text tokens as in Table 1.

During the pre-training phase, the visual encoder is frozen, allowing the optimization to be concentrated on the perceive sampler and the large language model. Initial weight for the perceive sampler and the large language model are sourced from BLIP2 [42] and InternLM [84], respectively. Given that the large language model lacks native understanding of image embeddings, its optimization within the framework of multimodal pre-training serves to enhance its capability to interpret such embeddings effectively. The training objective for the model centers on next-token prediction, utilizing cross-entropy loss function.

**Supervised Fine-tuning.** In the pre-training phase, image embeddings are aligned with language representations, equipping the large language model with a rudimentary understanding of image content. However, the model still lacks proficiency in utilizing the image information optimally. To address this limitation, we introduce a variety of vision-language tasks that the model undertakes during the subsequent Supervised Fine-Tuning Stage, which contains two consecutively steps, *i.e.*, *Multi-task training* and *Instruction tuning*.

*Multi-task Training.* As illustrated in Table 2, the multi-task training dataset is constructed from multiple sources to endow the model with a diverse range of capabilities, including scene understanding (*e.g.*, COCO Caption [12], SUB [62]), location understanding (*e.g.*, Visual Spatial Reasoning dataset [47]), optical character recognition (OCR) (*e.g.*, OCR-VQA [58]), and open-ended answering (*e.g.*, VQAv2 [2], GQA [34]), among others. Each of these tasks is formulated as a conversational interaction, adhering to the following format:

```
<|User|> : Instruction <eou>
<|Bot|> : Answer <eob>
```

where <eou> and <eob> represent the *end-of-user* and *end-of-bot* tokens, respectively. For VQA datasets with multiple questions per image, we structure them as multi-round conversations with randomly ordered questions, thereby substantially enhancing the efficiency of SFT.

In order to achieve stable and efficient fine-tuning, we retains the weights of the pre-existing large language model

<sup>1</sup>Due to copyright concerns, we will release the concept name list and source websites for the community to reproduce our concept data.

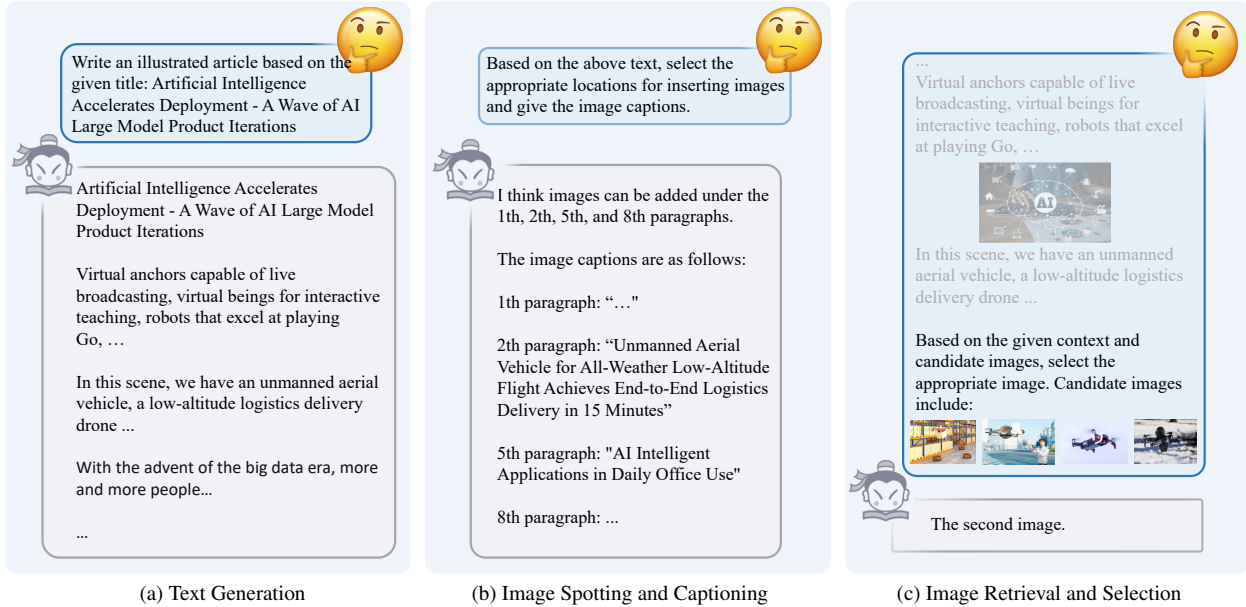


Figure 3. **The pipeline of the interleaved image-text composition.** (a) Given a writing instruction, the model initially generates a corresponding text-based article. (b) Subsequent to the article generation, the model is trained to identify suitable image locations and generate corresponding captions for the ensuing steps. (c) A text-image retrieval algorithm is initially employed to constrict the pool of candidate images. Following this, our model leverages its vision-language understanding ability to make the final image selection, ensuring thematic and visual coherence by considering both the preceding textual content and images within the article.

in a frozen state. Subsequently, we augment the architecture with Low-Rank Adaption (LoRA) [31] for the fine-tuning process. The perceive sampler is concurrently trained, albeit with a distinct learning rate.

*Instruction Tuning.* To further empower aforementioned model’s instruction following and interleaved image-text composition capability, as shown in Table 2, we utilize data from pure-text conversation corpora and LLaVA-150k for instruction-based tuning, and leverage the LRV dataset to mitigate hallucinations. The interleaved image-text composition dataset is constructed based on the methodology delineated in Section 3.3.

### 3.3. Interleaved Image-Text Composition

To craft interleaved image-text compositions, the initial step involves the generation of an article following human instruction. After this, accompanying illustrated images are incorporated at well-suited positions within the textual content, enriching the overall narrative and augmenting reader engagement. The pipeline of interleaved image-text composition is shown in Figure 3.

**Text Generation.** To facilitate the generation of extended text-based articles, we collect a dataset comprising interleaved image-text compositions from the Internet. To enable the model to generate text-based articles with respect to specific instructions, we utilize GPT-4 to generate diverse instructions based on the article, including a draft outline, a few keywords, or a simple title.

As mentioned in Section 1, a more engaging and immersive reading experience needs both text and suitable images. We empower our model with such composition capability with a decoupled pipeline, which defines the position and caption of images based on the generated text, and then selects the one image for each position from a list of candidates according to article context.

**Image Spotting and Captioning.** First, the acquired interleaved image-text data is leveraged to train our model for pinpointing image locations. For subsequent image retrieval, it’s imperative to generate an appropriate caption, enabling the application of various text-image retrieval algorithms. To mitigate this challenge, we generate caption data utilizing GPT-4, which is provided with the text-based article and image locations and is instructed to generate a caption for each image position that remains coherent with the overarching theme and concept.

**Image Retrieval and Selection.** Having obtained the captions, a variety of text-image retrieval methods become available for use. In this work, we opt for the CLIP model, capitalizing on its proven efficacy. We compute the similarity scores between the generated caption and each image in the candidate pool. The top  $m$  images, based on these similarity scores, are then selected to constitute the reduced candidate pool for further processing.

To guarantee thematic or conceptual coherence in the images dispersed throughout the article, we deploy our vision-language model to execute the final image selection. Our

Model	Overall	Exist.	Count	Pos.	Color	OCR	Poster	Cele.	Scene	Land.	Art.	Comm.	NumCal.	Trans.	Code	Avg.
MiniGPT-4[104]	694.3	68.3	55.0	43.3	43.3	57.5	41.8	54.4	71.8	54.0	60.5	59.3	45.0	0.0	40.0	49.6
LLaVA[50]	712.5	50.0	50.0	50.0	50.0	50.0	50.0	48.8	50.0	50.0	49.0	57.1	50.0	57.5	50.0	50.9
VisualGLM[24]	880.4	85.0	50.0	48.3	48.3	42.5	66.0	53.2	146.3	83.8	75.3	39.3	45.0	50.0	47.5	62.9
mPLUG-Owl[94]	1238.4	120.0	50.0	50.0	50.0	65.0	136.1	100.3	135.5	159.3	96.3	78.6	60.0	80.0	57.5	88.5
LLaMA-A-V2[27]	1194.9	120.0	50.0	48.3	48.3	<u>125.0</u>	99.7	86.2	148.5	150.3	69.8	81.4	62.5	50.0	55.0	85.4
InstructBLIP[18]	1417.9	185.0	143.3	66.7	66.7	72.5	123.8	101.2	153.0	79.8	<u>134.3</u>	129.3	40.0	65.0	57.5	101.3
Lynx[98]	1508.9	<u>195.0</u>	151.7	90.0	90.0	77.5	124.8	118.2	<u>164.5</u>	162.0	119.5	110.7	17.5	42.5	45.0	107.8
Otter[41]	1572.0	<u>195.0</u>	88.3	86.7	86.7	72.5	138.8	<u>172.7</u>	158.8	137.3	<u>129.0</u>	106.4	<u>72.5</u>	57.5	70.0	112.3
Chector[44]	1584.4	180.0	96.7	80.0	80.0	100.0	147.3	<u>164.1</u>	156.0	145.7	113.5	98.6	<u>77.5</u>	57.5	<u>87.5</u>	113.2
BLIVA[32]	1669.2	180.0	138.3	81.7	<u>180.0</u>	87.5	155.1	140.9	151.5	89.5	<u>133.3</u>	<u>136.4</u>	57.5	77.5	60.0	119.2
MMICL[102]	1810.7	170.0	<u>160.0</u>	81.7	156.7	100	146.3	141.8	153.8	136.1	<u>135.5</u>	<u>136.4</u>	<u>82.5</u>	<u>132.5</u>	<u>77.5</u>	129.3
LLaVA-1.5[49]	1826.7	185.0	<u>155.0</u>	<u>133.3</u>	<u>170.0</u>	125.0	<u>160.5</u>	<u>152.9</u>	<u>161.3</u>	<u>170.5</u>	117.7	127.8	42.5	77.5	47.5	130.5
Qwen-VL-Chat[4]	1848.3	158.3	150.0	<u>128.3</u>	<u>170.0</u>	<u>140.0</u>	<u>178.6</u>	120.6	152.3	<u>164.0</u>	125.5	130.7	40.0	<u>147.5</u>	42.5	132.0
Ours	<b>1919.5</b>	<u>190.0</u>	<u>158.3</u>	<u>126.7</u>	165.0	<u>125.0</u>	<u>161.9</u>	150.3	<u>159.8</u>	<u>165.3</u>	126.3	<u>138.6</u>	55.0	<u>112.5</u>	<u>85.0</u>	<b>137.1</b>

Table 3. **Evaluation of MME-Benchmark.** Here we report the results on all the sub tasks, including Existence(Exist.), Count, Position(Pos.), Color, OCR, Poster, Celebrity(Cele.), Scene, Landmark(Land.), Artwork(Art.), Commonsense Reasoning(Comm.), Numerical Calculation(NumCal.), Text Translation(Trans.), Code Reasoning(Code) and the task-level average (Avg.). We **bold** the *highest average / overall score* and highlight the *Top-3* model of each *sub task* with underline.

model selects images by considering both preceding text and prior images within the article. This mechanism enables the model to acquire an understanding of thematic and visual coherence, an expertise derived from the dataset of interleaved image-text compositions. Our model is also trained to select the ground-truth image from a candidate list given the article and image position to enhance the capability. The training data is directly structured from collected interleaved text-image articles and randomly selected negative candidates from the image repository.

## 4. Experiments

### 4.1. English-Based Benchmark results.

In this section, we validate the benchmark performance of our InternLM-XComposer after the Multi-task training. In the following, the comparison model is 7B version by default if there is no additional annotation.

**MME Benchmark**[26] measures the perception and cognition capability of multi-modality LLMs with carefully crafted questions within 14 sub-tasks. As shown in Table.3, our model reached a new state-of-the-art performance 137.11%, outperforms the previous method Qwen-VL-Chat with more than 5.0%. We also highlight the Top-3 models within each subtask with underline and we notice that our model reaches the Top-3 performance with 10 of the 14 sub-tasks. This proves the outstanding generalize of our model. **MMBench**[52] is a hand-crafted challenging benchmark, which evaluates the vision-related reasoning and perception capability with multi-choice questions. The MME Bench provides both a dev-set and test-set. Here we report the test-set performance of our model. As shown in Table.4. Our method gets 74.4% accuracy and outperforms previous methods by a large margin. Further, our model reaches the

Method	Avg.	LR	AR	RR	FP-S	FP-C	CP
MiniGPT-4[104]	23.0	13.6	32.9	8.9	28.8	11.2	28.3
VisualGLM [24]	33.5	11.4	48.8	27.7	35.8	17.6	41.5
InstructBLIP[18]	33.9	21.6	47.4	22.5	33.0	24.4	41.1
LLaVA [50]	36.2	15.9	53.6	28.6	41.8	20.0	40.4
LLaMA-A-V2 [27]	38.9	7.4	45.3	19.2	45.0	32.0	54.0
Otter-I [41]	48.3	22.2	63.3	39.4	46.8	36.4	60.6
LLaVA-1.5 [49]	59.5	32.4	72.6	49.3	62.3	52.2	67.7
Shikra [10]	60.2	33.5	69.6	53.1	61.8	50.4	71.7
Qwen-VL-Chat [4]	61.8	40.5	74.3	47.9	66.3	46.2	72.8
LMEye [46]	62.6	41.0	74.3	55.9	61.6	58.7	69.2
MMICL[101]	65.2	44.3	77.9	64.8	66.5	53.6	70.6
mPLUG-Owl[94]	66.0	43.4	76.0	62.1	68.6	55.9	73.0
Ours	<b>74.4</b>	<b>50.6</b>	<b>82.0</b>	<b>76.1</b>	<b>79.3</b>	<b>59.2</b>	<b>81.7</b>

Table 4. **Evaluation of MMBench test set.** Here we report the results on the six L-2 abilities, namely Logical Reasoning (LR), Attribute Reasoning (AR), Relation Reasoning (RR), Fine-grained Perception (Cross Instance) (FP-C), Fine-grained Perception (Single Instance) (FP-S), and Coarse Perception (CP).

best performance in all the dimensions. This proves that our model understands the image information well and can handle diverse vision-related tasks.

**Seed-Bench**[40] is a large-scale multi-modality benchmark, which is built with the help of GPT-4 and contains nearly 19K multi-choice questions for both image and video. Here we report the image-set results in Table.5. It can be observed that our model gets the best overall performance and the highest performance in 6 of the 9 sub-tasks. We also notice that the sub-task data number is in-balance, so the overall metric would be biased toward some sub-tasks. To better evaluate the generalized capability of the LLMs along different tasks. We also report the task-level average, and our model reaches the state-of-the-art average

Method	Language Model	Overall	T-Avg.	Sense.U	Inst.Id	Inst.At	Inst.Lo	Inst.Co	Spat.R	Inst.It	Vis.R	Text.R
OpenFlamingo[3]	MPT-7B	42.7	39.4	53.2	45.3	40	31.2	39.3	32.6	36.1	51.4	25.9
Otter[41]	MPT-7B	42.9	40.08	51.3	43.5	42.3	34.2	38.4	30.9	40.2	55.3	24.7
MiniGPT-4[104]	Vicuna-7B	47.4	42.6	56.3	49.2	45.8	37.9	45.3	32.6	47.4	57.1	11.8
BLIP-2 [43]	Flan-T5-XL	49.7	45.7	59.1	53.9	49.2	42.3	43.2	36.7	55.7	45.6	25.9
IDEFICS-80b-instruct[39]	LLaMA-65B	53.2	54.4	64	52.6	50.8	48.3	46.1	45.5	62.9	68	51.8
Kosmos-2[65]	Kosmos 1.3B	54.4	49.4	63.4	57.1	58.5	44	41.4	37.9	55.7	60.7	25.9
InstructBLIP-Vicuna[18]	Vicuna-7B	58.8	52.2	60.2	58.9	65.6	43.6	<b>57.2</b>	40.3	52.6	47.7	43.5
Qwen-VL-Chat[4]	Qwen-7B	65.4	61.9	73.3	67.3	<b>69.6</b>	57.7	52.9	48.2	59.8	74.6	<b>53.5</b>
LLaVA-1.5 [49]	LLaMA2-7B	66.2	61.8	74.3	69.9	67.6	60.3	<b>57.2</b>	50.8	63.9	77.3	35.3
Ours	InternLM-7B	<b>66.9</b>	<b>65.2</b>	<b>75.0</b>	<b>71.7</b>	67.6	<b>60.8</b>	56.2	<b>55.3</b>	<b>74.4</b>	<b>77.0</b>	48.5

Table 5. **Evaluation of Seed-Bench test set.** Here we report the results on the image-based sub tasks, including Scene Understanding(Sense.U), Instance Identity(Inst.Id), Instance Attributes(Inst.At), Instance Localization(Inst.Lo), Instance Counting(Inst.Co), Spatial Relation(Spat.R), Instance Interaction(Inst.It), Visual Reasoning(Vis.R), Text Recognition(Text.R), and both overall accuracy(Overall) and task-level average accuracy(T-Avg.)

Method	Overall	Perception	Description	Assesment
VisualGLM[24]	42.4	53.3	49.8	24.0/23.9
Otter [41]	46.7	47.2	60.2	32.3/33.3
MiniGPT-4[104]	47.5	51.8	61.2	29.3/30.0
InstructBLIP[18]	48.3	55.8	47.3	38.9/44.6
Shikra [10]	48.3	55.3	55.7	33.6/34.5
LLaMA-A-V2 [27]	51.8	58.1	57.5	38.1/41.7
LLaVA[50]	54.4	54.7	62.7	44.4/47.4
LLaVA-v1.5[49]	55.0	61.4	57.8	44.4/47.4
Qwen-VL-Chat[4]	55.6	61.7	56.0	47.5/50.6
mPLUG-Owl[94]	56.4	58.9	65.7	43.2/45.8
Ours	<b>63.6</b>	<b>64.4</b>	<b>70.2</b>	<b>54.2/58.1</b>

Table 6. **Evaluation of Q-Bench test set.** Here we report all the sub-tasks, including Perception, Description and Assessment. For Assessment, we report both SRCC and PLCC score.

accuracy and outperforms the previous method with 3.3%. This further proves the general capability of our model.

**Q-Bench**[90] is a comprehensive benchmark which focus on the low-level vision, including three realms: perception, description, and assessment. Here we report the test set results in Table.6. Our model shows the state-of-the-art performance on all the three tasks, surpass previous methods with a large margin. The results suggest our model has a comprehensive understanding of the image, which not only focus the high-level semantic feature of the image, but also the low-level information.

## 4.2. Chinese-Based Benchmark results.

As we introduced in Sec.1, our model is pretrained with rich multilingual knowledge. To prove the effectiveness of the pretraining, here we further evaluate its performance with two Chinese-based benchmarks.

**MMBench-CN**[52] is the Chinese translated benchmark of the original MMBench, which shows the vision-related Chinese understanding and reasoning capability. Here we report the test-set performance in Table.7. It can be observed that our method outperforms previous methods by a large

Method	Avg	LR	AR	RR	FP-S	FP-C	CP
OpenFlamingo[3]	1.7	1.7	4.5	0	1.5	0.8	1.3
MiniGPT-4[104]	11.9	11.6	19.4	5.7	14.6	6.5	10.9
InstructBLIP[18]	23.9	9.2	38.5	16.6	20.9	15	30.8
mPLUG-Owl[94]	24.9	6.9	34	17.5	33.4	8.5	30.6
VisualGLM[24]	25.6	5.2	42	18	24.1	13	34.5
LLaVA[50]	36.6	15	52.4	17.1	34.4	27.5	50.3
IDEFICS-80B-I[39]	38.1	20.8	49	27.5	29.1	36.0	51.2
LLaVA-1.5[49]	53.8	31.2	67.7	42.7	49.5	43.7	67.7
Qwen-VL-Chat[4]	56.3	35.3	63.5	46	63.6	43.7	64.7
Ours	<b>72.4</b>	<b>44.5</b>	<b>79.5</b>	<b>83.4</b>	<b>71.6</b>	<b>56.3</b>	<b>82.4</b>

Table 7. **Evaluation of MMBench-CN test set.** Here we report the results on the six L-2 abilities based on Chinese.

Method	Avg	CP	CR	F&C	HF	S&B	SR	TS
OpenFlamingo[3]	0.7	1.8	0	0.8	0.0	0.0	2.2	1.5
MiniGPT-4[104]	1.7	7.0	4.0	0.0	0.0	1.0	0.0	0.0
LLaVA[50]	8.3	10.5	8.1	7.6	1.7	8.0	11.1	10.6
VisualGLM[24]	9.2	14.0	11.1	8.4	0.0	14.0	4.4	7.6
InstructBLIP[18]	12.1	8.8	9.1	21.0	0.0	12.0	6.7	18.2
mPLUG-Owl[94]	12.9	22.8	17.2	6.7	0.0	25.0	4.4	7.6
LLaVA-1.5[49]	16.4	15.8	19.2	10.9	3.4	21.0	37.8	12.1
Qwen-VL-Chat[4]	39.3	40.4	33.3	31.9	3.4	<b>67.0</b>	51.1	42.4
Ours	<b>47.6</b>	<b>50.9</b>	<b>53.5</b>	<b>42.0</b>	<b>10.3</b>	55.0	<b>73.3</b>	<b>50.0</b>

Table 8. **Evaluation of CCBench test set.** We report all the sub-tasks, including Calligraphy Painting(CP), Cultural Relic(CR), Food & Clothes(F&C), Historical Figures(H&F), Scenery & Building(S&B), Sketch Reasoning(SR), Traditional Show(TS),

margin. When comparing with the English version performance in Table.4. Qwen and VisualGLM have 4.9% and 7.9% performance degrading, while the performance gap of our model between different languages is only 2.0%. This proves the strong multi-lingo capability of our model.

**Chinese-Bench**[52] is a Chinese knowledge-related benchmark, that challenges the model with Chinese traditional cultural questions, including art, food, clothes, landmarks, etc. The performance is given in Table.8. It can be observed that the benchmark is quite challenging, most LLaMA-based model fails to answer these questions, due

Method	Human Evaluation				GPT4-Vision Evaluation			
	Avg.	Pref.	Text	Image	Avg.	Pref.	Text	Image
Qwen-14B[66]	0.62	0.52	0.80	0.54	0.82	0.78	0.91	0.72
Intern-20B[84]	0.64	0.54	0.82	0.56	0.81	0.82	0.89	0.70
GPT3.5 [60]	0.71	0.64	0.88	0.59	0.84	0.84	0.91	0.75
Ours	0.74	0.65	0.90	<b>0.67</b>	0.87	<b>0.90</b>	0.93	<b>0.79</b>
GPT4-V [61]	<b>0.77</b>	<b>0.73</b>	<b>0.95</b>	0.64	<b>0.89</b>	0.88	<b>0.96</b>	0.78

Table 9. Quantitative results by human and GPT-4Vision. **Text** means the writing-related scores and **Image** means the image-selection related scores. The evaluation by human and GPT-4Vision shows consist conclusion that GPT-4 performs best and our model is on par with the GPT3.5, better than other LLMs.

Method	Human	Top-1	GPT4-Vision	Our
Score	100.0	40.2	51.7	80.4

Table 10. Effectiveness of Image Selection, **Human** is the ground truth selected by human.

to the lack of corresponding knowledge. Compared with LLaMA-based methods, the Qwen-based model Qwen-VL-Chat shows a much better performance of 39.3%. While it is still worse than InternLM-based model, which reaches a new state-of-the-art performance of 47.6%. This proves the rich Chinese knowledge of InternLM and the great alignment between the vision and language knowledge by our large-scale pre-training.

### 4.3. Interleaved Image-Text Composition

**Quantitative results.** Due to the lack of existing metrics to evaluate the image-text interleaved article quality, we designed a detailed user study metric<sup>2</sup>, including eight dimensions: four text-related dimensions (instruction following, writing quality, logic, factualness), three image-related dimensions (image-text consistency, image informative, image consistency), and one subjective preference. As our InternLM-XComposer is the first interleaved image-text composition model, we compare the composition quality with recent leading LLMs and VLMs, including GPT4-V, GPT3.5, InternLM-20B, and Qwen-14B. For a fair comparison, we apply a similar composition pipeline as mentioned in Sec.3.3 in these solutions. Notably, the image selection phase is not supported in language-only models (GPT3.5, InternLM-20B, and Qwen-14B), in which retrieved images with top-1 similarity are adopted as the final illustrations. In practice, we generated articles with 20 articles. For robustness and reliability of final results, we adopt both human evaluation and GPT4-V scoring. Specifically, we invite 10 human experts for assessment. In the meantime, GPT4-V also rates scores for these articles on the proposed eight dimensions.

As presented in Table.9, GPT-4V shows the best performance in all the text-related dimensions and the highest

<sup>2</sup>Please refer to the supplementary materials for more details.

Method	MME	MMBench	Seed Bench
Ours	1919.5	74.4	66.9
Freeze Perceive Sampler	1819.1	71.3	63.2
Freeze Attention LoRA	1776.5	72.0	65.9
Freeze FFN LoRA	1828.7	72.4	66.4

Table 11. Ablation on Learnable Components.

LLM Backbone	MME	MMBench	MMBench-CN	CCBench
LLaMA-2 [86]	1895.9	72.6	66.7	44.6
InternLM[84]	1919.5	74.4	72.4	47.6

Table 12. Ablation on LLM Backbone.

overall score. Benefiting from the interleaved image-text composition training, our InternLM-XComposer performs the best on image-related dimensions and the second best on the text-related dimensions and average score.

**Effectiveness of Image Selection** The last step of our interleaved Image-Text composition pipeline is the Image retrieval and selection. The InternLM-XComposer could select a proper image from the retrieved candidates based on the context. Here we study the effectiveness of the image selection based on human preference. Specifically, we provide the text and candidate images to human experts, GPT4-Vision and Intern-XComposer, and use the human-selected images as the ground truth. We also use the image with the highest retrieval similarity as the ‘Top-1’ baseline. As shown in Table.10, InternLM-XComposer gets a higher score than GPT4- V, which means the image selected by our model is more consistent with the human preference.

**Qualitative results.** We direct readers to the supplementary materials for detailed qualitative results of the interleaved image-text compositions and multimodal conversations generated by the InternLM-XComposer.

### 4.4. Ablation Study

**Learnable Components.** Here we study the influence of different learnable components in the multi-task supervised fine-tuning stage. As shown in Table.11, the Perceive Sampler is critical for the multi-task learning, which shows significant influence on most benchmarks. For the LoRA in LLM, the Attention and FFN part are also important to realize a superb performance.

**LLM selection.** Then we study the influence of different LLMs, here we consider the InternLM-7B and LLaMA2-7B, with the same pre-training and supervised fine-tuning strategy. Here we report the results on MME, MMBench, MMBench-CN and CCBench. With the results in Table.12, we find the LLaMA-2 performs similar with InternLM-7B in the English-based benchmarks, while the performances gap is enlarged in the Chinese-based benchmarks.



## 5. Conclusion

In this paper, we present InternLM-XComposer, a vision-language large model with superb multi-modality understanding and composition capability. Benefiting from the rich multi-lingual and multi-modality knowledge from carefully designed pretraining, our model could generate coherent interleaved image-text composition, and shows state-of-the-art performance across various vision-language LLM benchmarks. We hope XComposer could provide new insight for the advanced vision-language interaction.

## References

- [1] Jean-Baptiste Alayrac, Jeff Donahue, Pauline Luc, Antoine Miech, Iain Barr, Yana Hasson, Karel Lenc, Arthur Mensch, Katie Millican, Malcolm Reynolds, Roman Ring, Eliza Rutherford, Serkan Cabi, Tengda Han, Zhitao Gong, Sina Samangooei, Marianne Monteiro, Jacob Menick, Sebastian Borgeaud, Andrew Brock, Aida Nematzadeh, Sahand Sharifzadeh, Mikolaj Binkowski, Ricardo Barreira, Oriol Vinyals, Andrew Zisserman, and Karen Simonyan. Flamingo: a visual language model for few-shot learning, 2022. [3](#)
- [2] Stanislaw Antol, Aishwarya Agrawal, Jiasen Lu, Margaret Mitchell, Dhruv Batra, C. Lawrence Zitnick, and Devi Parikh. Vqa: Visual question answering. In *International Conference on Computer Vision (ICCV)*, 2015. [4](#)
- [3] Anas Awadalla, Irena Gao, Josh Gardner, Jack Hessel, Yusuf Hanafy, Wanrong Zhu, Kalyani Marathe, Yonatan Bitton, Samir Gadre, Shiori Sagawa, Jenia Jitsev, Simon Kornblith, Pang Wei Koh, Gabriel Ilharco, Mitchell Wortsman, and Ludwig Schmidt. Openflamingo: An open-source framework for training large autoregressive vision-language models. *arXiv.org*, 2023. [3](#), [7](#)
- [4] Jinze Bai, Shuai Bai, Shusheng Yang, Shijie Wang, Sinan Tan, Peng Wang, Junyang Lin, Chang Zhou, and Jingren Zhou. Qwen-vl: A frontier large vision-language model with versatile abilities. *arXiv.org*, 2023. [3](#), [6](#), [7](#), [17](#)
- [5] Baichuan. Baichuan 2: Open large-scale language models. *arXiv.org*, 2023. [2](#), [3](#)
- [6] James Betker, Gabriel Goh, Li Jing, Tim Brooks, Jianfeng Wang, Linjie Li, Long Ouyang, Juntang Zhuang, Joyce Lee, Yufei Guo, Wesam Manassra, Prafulla Dhariwal, Casey Chu, Yunxin Jiao, and Aditya Ramesh. Improving image generation with better captions. [2](#)
- [7] Tom Brown, Benjamin Mann, Nick Ryder, Melanie Subbiah, Jared D Kaplan, Prafulla Dhariwal, Arvind Neelakantan, Pranav Shyam, Girish Sastry, Amanda Askell, et al. Language models are few-shot learners. *Advances in Neural Information Processing Systems (NeurIPS)*, 33:1877–1901, 2020. [2](#), [3](#)
- [8] Soravit Changpinyo, Piyush Sharma, Nan Ding, and Radu Soricut. Conceptual 12m: Pushing web-scale image-text pre-training to recognize long-tail visual concepts. In *Proceedings of the IEEE/CVF Conference on Computer Vision and Pattern Recognition*, pages 3558–3568, 2021. [2](#), [4](#)
- [9] Jun Chen, Deyao Zhu, Xiaoqian Shen, Xiang Li, Zechu Liu, Pengchuan Zhang, Raghuraman Krishnamoorthi, Vikas Chandra, Yunyang Xiong, and Mohamed Elhoseiny. Minigt-v2: large language model as a unified interface for vision-language multi-task learning. *arXiv preprint arXiv:2310.09478*, 2023. [3](#)
- [10] Keqin Chen, Zhao Zhang, Weili Zeng, Richong Zhang, Feng Zhu, and Rui Zhao. Shikra: Unleashing multimodal llm’s referential dialogue magic. *arXiv.org*, 2023. [3](#), [6](#), [7](#)
- [11] Xi Chen, Josip Djolonga, Piotr Padlewski, Basil Mustafa, Soravit Changpinyo, Jialin Wu, Carlos Riquelme Ruiz, Sebastian Goodman, Xiao Wang, Yi Tay, Siamak Shakeri, Mostafa Dehghani, Daniel Salz, Mario Lucic, Michael Tschannen, Arsha Nagrani, Hexiang Hu, Mandar Joshi, Bo Pang, Ceslee Montgomery, Paulina Pietrzyk, Marvin Ritter, AJ Piergiovanni, Matthias Minderer, Filip Pavetic, Austin Waters, Gang Li, Ibrahim Alabdulmohsin, Lucas Beyer, Julien Amelot, Kenton Lee, Andreas Peter Steiner, Yang Li, Daniel Keysers, Anurag Arnab, Yuanzhong Xu, Keran Rong, Alexander Kolesnikov, Mojtaba Seyedhosseini, Anelia Angelova, Xiaohua Zhai, Neil Houlsby, and Radu Soricut. Pali-x: On scaling up a multilingual vision and language model, 2023. [3](#)
- [12] Xinlei Chen, Hao Fang, Tsung-Yi Lin, Ramakrishna Vedantam, Saurabh Gupta, Piotr Dollar, and C. Lawrence Zitnick. Microsoft coco captions: Data collection and evaluation server, 2015. [4](#)
- [13] Xi Chen, Xiao Wang, Lucas Beyer, Alexander Kolesnikov, Jialin Wu, Paul Voigtlaender, Basil Mustafa, Sebastian Goodman, Ibrahim Alabdulmohsin, Piotr Padlewski, Daniel Salz, Xi Xiong, Daniel Vlasic, Filip Pavetic, Keran Rong, Tianli Yu, Daniel Keysers, Xiaohua Zhai, and Radu Soricut. Pali-3 vision language models: Smaller, faster, stronger, 2023. [3](#)
- [14] Xi Chen, Xiao Wang, Soravit Changpinyo, AJ Piergiovanni, Piotr Padlewski, Daniel Salz, Sebastian Goodman, Adam Grycner, Basil Mustafa, Lucas Beyer, Alexander Kolesnikov, Joan Puigcerver, Nan Ding, Keran Rong, Hassan Akbari, Gaurav Mishra, Linting Xue, Ashish Thapliyal, James Bradbury, Weicheng Kuo, Mojtaba Seyedhosseini, Chao Jia, Burcu Karagol Ayan, Carlos Riquelme, Andreas Steiner, Anelia Angelova, Xiaohua Zhai, Neil Houlsby, and Radu Soricut. Pali: A jointly-scaled multilingual language-image model, 2023. [3](#)
- [15] Wei-Lin Chiang, Zhuohan Li, Zi Lin, Ying Sheng, Zhanghao Wu, Hao Zhang, Lianmin Zheng, Siyuan Zhuang, Yonghao Zhuang, Joseph E. Gonzalez, Ion Stoica, and Eric P. Xing. Vicuna: An open-source chatbot impressing gpt-4 with 90%\* chatgpt quality, March 2023. [2](#), [3](#), [4](#)
- [16] Aakanksha Chowdhery, Sharan Narang, Jacob Devlin, Maarten Bosma, Gaurav Mishra, Adam Roberts, Paul Barham, Hyung Won Chung, Charles Sutton, Sebastian Gehrmann, et al. Palm: Scaling language modeling with pathways. *arXiv.org*, 2022. [2](#), [3](#)
- [17] Yin Cui, Menglin Jia, Tsung-Yi Lin, Yang Song, and Serge Belongie. Class-balanced loss based on effective number of samples. In *CVPR*, Jun 2019. [2](#)
- [18] Wenliang Dai, Junnan Li, Dongxu Li, Anthony Meng Huat Tiong, Junqi Zhao, Weisheng Wang, Boyang Li, Pascale Fung, and Steven Hoi. Instructblip: Towards general-purpose vision-language models with instruction tuning,

2023. [2](#), [3](#), [6](#), [7](#), [17](#)
- [19] Abhishek Das, Satwik Kottur, Khushi Gupta, Avi Singh, Deshraj Yadav, José MF Moura, Devi Parikh, and Dhruv Batra. Visual dialog. In *Proceedings of the IEEE conference on computer vision and pattern recognition*, pages 326–335, 2017. [4](#)
- [20] Jia Deng, Wei Dong, Richard Socher, Li-Jia Li, Kai Li, and Li Fei-Fei. Imagenet: A large-scale hierarchical image database. In *Proceedings of the IEEE/CVF Conference on Computer Vision and Pattern Recognition (CVPR)*, pages 248–255, 2009. [3](#)
- [21] Jacob Devlin, Ming-Wei Chang, Kenton Lee, and Kristina Toutanova. Bert: Pre-training of deep bidirectional transformers for language understanding. *arXiv.org*, 2018. [3](#)
- [22] Runpei Dong, Chunrui Han, Yuang Peng, Zekun Qi, Zheng Ge, Jinrong Yang, Liang Zhao, Jianjian Sun, Hongyu Zhou, Haoran Wei, Xiangwen Kong, Xiangyu Zhang, Kaisheng Ma, and Li Yi. Dreamllm: Synergistic multimodal comprehension and creation. *arXiv preprint arXiv:2309.11499*, 2023. [3](#)
- [23] Danny Driess, Fei Xia, Mehdi S. M. Sajjadi, Corey Lynch, Aakanksha Chowdhery, Brian Ichter, Ayzaan Wahid, Jonathan Tompson, Quan Vuong, Tianhe Yu, Wenlong Huang, Yevgen Chebotar, Pierre Sermanet, Daniel Duckworth, Sergey Levine, Vincent Vanhoucke, Karol Hausman, Marc Toussaint, Klaus Greff, Andy Zeng, Igor Mordatch, and Pete Florence. Palm-e: An embodied multimodal language model. In *arXiv preprint arXiv:2303.03378*, 2023. [2](#), [3](#)
- [24] Zhengxiao Du, Yujie Qian, Xiao Liu, Ming Ding, Jiezhong Qiu, Zhilin Yang, and Jie Tang. Glm: General language model pretraining with autoregressive blank infilling. In *Proceedings of the 60th Annual Meeting of the Association for Computational Linguistics (Volume 1: Long Papers)*, pages 320–335, 2022. [2](#), [3](#), [6](#), [7](#), [17](#)
- [25] Yuxin Fang, Wen Wang, Binhui Xie, Quan Sun, Ledell Wu, Xinggang Wang, Tiejun Huang, Xinlong Wang, and Yue Cao. Eva: Exploring the limits of masked visual representation learning at scale. In *Proceedings of the IEEE/CVF Conference on Computer Vision and Pattern Recognition (CVPR)*, pages 19358–19369, 2023. [3](#)
- [26] Chaoyou Fu, Peixian Chen, Yunhang Shen, Yulei Qin, Mengdan Zhang, Xu Lin, Zhenyu Qiu, Wei Lin, Jinrui Yang, Xiawu Zheng, Ke Li, Xing Sun, and Rongrong Ji. Mme: A comprehensive evaluation benchmark for multimodal large language models. *arXiv preprint arXiv:2306.13394*, 2023. [2](#), [6](#)
- [27] Peng Gao, Jiaming Han, Renrui Zhang, Ziyi Lin, Shijie Geng, Aojun Zhou, W. Zhang, Pan Lu, Conghui He, Xiangyu Yue, Hongsheng Li, and Yu Jiao Qiao. Llama-adapter v2: Parameter-efficient visual instruction model. *ArXiv*, abs/2304.15010, 2023. [6](#), [7](#), [17](#)
- [28] Yuying Ge, Yixiao Ge, Ziyun Zeng, Xintao Wang, and Ying Shan. Planting a seed of vision in large language model. [3](#)
- [29] Jiayi Gu, Xiaojun Meng, Guansong Lu, Lu Hou, Niu Minzhe, Xiaodan Liang, Lewei Yao, Runhui Huang, Wei Zhang, Xin Jiang, et al. Wukong: A 100 million large-scale chinese cross-modal pre-training benchmark. *Advances in Neural Information Processing Systems*, 35:26418–26431, 2022. [4](#)
- [30] Conghui He, Zhenjiang Jin, Chaoxi Xu, Jiantao Qiu, Bin Wang, Wei Li, Hang Yan, Jiaqi Wang, and Da Lin. Wanjuan: A comprehensive multimodal dataset for advancing english and chinese large models. *ArXiv*, abs/2308.10755, 2023. [4](#), [14](#)
- [31] Edward J Hu, Yelong Shen, Phillip Wallis, Zeyuan Allen-Zhu, Yuanzhi Li, Shean Wang, Lu Wang, and Weizhu Chen. LoRA: Low-rank adaptation of large language models. In *International Conference on Learning Representations*, 2022. [5](#), [14](#)
- [32] W. Hu, Y. Xu, Y. Li, W. Li, Z. Chen, and Z. Tu. Bliva: A simple multimodal llm for better handling of text-rich visual questions. *ArXiv*, abs/2308.09936, 2023. [6](#)
- [33] Ziniu Hu, Ahmet Iscen, Chen Sun, Zirui Wang, Kai-Wei Chang, Yizhou Sun, Cordelia Schmid, David A Ross, and Alireza Fathi. Reveal: Retrieval-augmented visual-language pre-training with multi-source multimodal knowledge memory. In *Proceedings of the IEEE/CVF Conference on Computer Vision and Pattern Recognition (CVPR)*, pages 23369–23379, 2023. [3](#)
- [34] Drew A Hudson and Christopher D Manning. Gqa: A new dataset for real-world visual reasoning and compositional question answering. *Conference on Computer Vision and Pattern Recognition (CVPR)*, 2019. [4](#)
- [35] Chao Jia, Yinfei Yang, Ye Xia, Yi-Ting Chen, Zarana Parekh, Hieu Pham, Quoc Le, Yun-Hsuan Sung, Zhen Li, and Tom Duerig. Scaling up visual and vision-language representation learning with noisy text supervision. In *Proceedings of the International Conference on Machine Learning (ICML)*, pages 4904–4916. PMLR, 2021. [3](#)
- [36] Albert Q. Jiang, Alexandre Sablayrolles, Arthur Mensch, Chris Bamford, Devendra Singh Chaplot, Diego de las Casas, Florian Bressand, Gianna Lengyel, Guillaume Lample, Lucile Saulnier, Léo Renard Lavaud, Marie-Anne Lachaux, Pierre Stock, Teven Le Scao, Thibaut Lavril, Thomas Wang, Timothée Lacroix, and William El Sayed. Mistral 7b, 2023. [3](#)
- [37] Jing Yu Koh, Ruslan Salakhutdinov, and Daniel Fried. Grounding language models to images for multimodal inputs and outputs. 2023. [3](#)
- [38] Andreas Köpf, Yannic Kilcher, Dimitri von Rütte, Sotiris Anagnostidis, Zhi-Rui Tam, Keith Stevens, Abdullah Barhoum, Nguyen Minh Duc, Oliver Stanley, Richárd Nagyfi, Shahul ES, Sameer Suri, David Glushkov, Arnav Dantuluri, Andrew Maguire, Christoph Schuhmann, Huu Nguyen, and Alexander Mattick. Openassistant conversations – democratizing large language model alignment, 2023. [4](#)
- [39] Hugo Laurençon, Lucile Saulnier, Léo Tronchon, Stas Bekman, Amanpreet Singh, Anton Lozhkov, Thomas Wang, Siddharth Karamcheti, Alexander M. Rush, Douwe Kiela, Matthieu Cord, and Victor Sanh. Obelics: An open web-scale filtered dataset of interleaved image-text documents, 2023. [7](#)
- [40] Bohao Li, Rui Wang, Guangzhi Wang, Yuying Ge, Yixiao Ge, and Ying Shan. Seed-bench: Benchmarking multimodal llms with generative comprehension, 2023. [2](#), [6](#)
- [41] Bo Li, Yuanhan Zhang, Liangyu Chen, Jinghao Wang,

- Jingkang Yang, and Ziwei Liu. Otter: A multi-modal model with in-context instruction tuning. *arXiv.org*, 2023. 3, 6, 7, 17
- [42] Junnan Li, Dongxu Li, Silvio Savarese, and Steven C. H. Hoi. Blip-2: Bootstrapping language-image pre-training with frozen image encoders and large language models. *ArXiv*, abs/2301.12597, 2023. 2, 3, 4, 17
- [43] Junnan Li, Dongxu Li, Caiming Xiong, and Steven Hoi. Blip: Bootstrapping language-image pre-training for unified vision-language understanding and generation. In *Proceedings of the International Conference on Machine Learning (ICML)*, pages 12888–12900. PMLR, 2022. 3, 7
- [44] Juncheng Li, Kaihang Pan, Zhiqi Ge, Minghe Gao, Hanwang Zhang, Wei Ji, Wenqiao Zhang, Tat-Seng Chua, Siliang Tang, and Yueting Zhuang. Empowering vision-language models to follow interleaved vision-language instructions. *ArXiv*, abs/2308.04152, 2023. 6
- [45] Liunian Harold Li\*, Pengchuan Zhang\*, Haotian Zhang\*, Jianwei Yang, Chunyuan Li, Yiwu Zhong, Lijuan Wang, Lu Yuan, Lei Zhang, Jenq-Neng Hwang, Kai-Wei Chang, and Jianfeng Gao. Grounded language-image pre-training. In *Proceedings of the IEEE/CVF Conference on Computer Vision and Pattern Recognition (CVPR)*, 2022. 3
- [46] Yunxin Li, Baotian Hu, Xinyu Chen, Lin Ma, Yong Xu, and Min Zhang. Lmeyer: An interactive perception network for large language models, 2023. 6
- [47] Fangyu Liu, Guy Edward Toh Emerson, and Nigel Collier. Visual spatial reasoning. *Transactions of the Association for Computational Linguistics*, 2023. 4
- [48] Fuxiao Liu, Kevin Lin, Linjie Li, Jianfeng Wang, Yaser Yacoob, and Lijuan Wang. Aligning large multi-modal model with robust instruction tuning. *arXiv preprint arXiv:2306.14565*, 2023. 4
- [49] Haotian Liu, Chunyuan Li, Yuheng Li, and Yong Jae Lee. Improved baselines with visual instruction tuning. *arXiv preprint arXiv:2310.03744*, 2023. 6, 7, 17
- [50] Haotian Liu, Chunyuan Li, Qingyang Wu, and Yong Jae Lee. Visual instruction tuning. *arXiv.org*, 2023. 2, 3, 4, 6, 7, 17
- [51] Shilong Liu, Zhaoyang Zeng, Tianhe Ren, Feng Li, Hao Zhang, Jie Yang, Chunyuan Li, Jianwei Yang, Hang Su, Jun Zhu, et al. Grounding dino: Marrying dino with grounded pre-training for open-set object detection. *arXiv.org*, 2023. 3
- [52] Yuan Liu, Haodong Duan, Yuanhan Zhang, Bo Li, Songyang Zhnag, Wangbo Zhao, Yike Yuan, Jiaqi Wang, Conghui He, Ziwei Liu, Kai Chen, and Dahua Lin. Mmbench: Is your multi-modal model an all-around player? *arXiv:2307.06281*, 2023. 2, 6, 7
- [53] Yulong Liu, Guibo Zhu, Bin Zhu, Qi Song, Guojing Ge, Haoran Chen, GuanHui Qiao, Ru Peng, Lingxiang Wu, and Jinqiao Wang. Taisu: A 166m large-scale high-quality dataset for chinese vision-language pre-training. *Advances in Neural Information Processing Systems*, 35:16705–16717, 2022. 4
- [54] Ziwei Liu, Zhongqi Miao, Xiaohang Zhan, Jiayun Wang, Boqing Gong, and Stella X. Yu. Large-scale long-tailed recognition in an open world. In *CVPR*, Jun 2019. 2
- [55] Pan Lu, Swaroop Mishra, Tanglin Xia, Liang Qiu, Kai-Wei Chang, Song-Chun Zhu, Oyvind Tafjord, Peter Clark, and Ashwin Kalyan. Learn to explain: Multimodal reasoning via thought chains for science question answering. *Advances in Neural Information Processing Systems*, 35:2507–2521, 2022. 4
- [56] Pan Lu, Liang Qiu, Jiaqi Chen, Tony Xia, Yizhou Zhao, Wei Zhang, Zhou Yu, Xiaodan Liang, and Song-Chun Zhu. Iconqa: A new benchmark for abstract diagram understanding and visual language reasoning. *arXiv preprint arXiv:2110.13214*, 2021. 4
- [57] Kenneth Marino, Mohammad Rastegari, Ali Farhadi, and Roozbeh Mottaghi. Ok-vqa: A visual question answering benchmark requiring external knowledge. In *Proceedings of the IEEE/cvf conference on computer vision and pattern recognition*, pages 3195–3204, 2019. 4
- [58] Anand Mishra, Shashank Shekhar, Ajeet Kumar Singh, and Anirban Chakraborty. Ocr-vqa: Visual question answering by reading text in images. In *ICDAR*, 2019. 4
- [59] MEJ Newman. Power laws, pareto distributions and zipf’s law. *Contemporary Physics*, page 323–351, Sep 2005. 2
- [60] OpenAI. Chatgpt. <https://openai.com/blog/chatgpt>, 2022. 2, 3, 8
- [61] OpenAI. Gpt-4 technical report, 2023. 2, 8
- [62] Vicente Ordonez, Girish Kulkarni, and Tamara L. Berg. Im2text: Describing images using 1 million captioned photographs. In *Neural Information Processing Systems (NIPS)*, 2011. 2, 4
- [63] Long Ouyang, Jeffrey Wu, Xu Jiang, Diogo Almeida, Carroll Wainwright, Pamela Mishkin, Chong Zhang, Sandhini Agarwal, Katarina Slama, Alex Ray, et al. Training language models to follow instructions with human feedback. *Advances in Neural Information Processing Systems (NeurIPS)*, 35:27730–27744, 2022. 3
- [64] Guilherme Penedo, Quentin Malartic, Daniel Hesslow, Ruxandra Cojocar, Alessandro Cappelli, Hamza Alobeidli, Baptiste Pannier, Ebtesam Almazrouei, and Julien Launay. The refinedweb dataset for falcon llm: Outperforming curated corpora with web data, and web data only, 2023. 3
- [65] Zhiliang Peng, Wenhui Wang, Li Dong, Yaru Hao, Shaohan Huang, Shuming Ma, and Furu Wei. Kosmos-2: Grounding multimodal large language models to the world. *arXiv.org*, 2023. 3, 7
- [66] Qwen. Introducing qwen-7b: Open foundation and human-aligned models (of the state-of-the-arts), 2023. 2, 3, 8
- [67] Alec Radford, Jong Wook Kim, Chris Hallacy, Aditya Ramesh, Gabriel Goh, Sandhini Agarwal, Girish Sastry, Amanda Askell, Pamela Mishkin, Jack Clark, et al. Learning transferable visual models from natural language supervision. In *Proceedings of the International Conference on Machine Learning (ICML)*, pages 8748–8763. PMLR, 2021. 2, 3, 15
- [68] Alec Radford, Karthik Narasimhan, Tim Salimans, Ilya Sutskever, et al. Improving language understanding by generative pre-training. 2018. 3
- [69] Colin Raffel, Noam Shazeer, Adam Roberts, Katherine Lee, Sharan Narang, Michael Matena, Yanqi Zhou, Wei Li, and Peter J Liu. Exploring the limits of transfer learning with a unified text-to-text transformer. *Journal of Machine Learning Research (JMLR)*, 21(1):5485–5551, 2020. 2, 3

- [70] Aditya Ramesh, Prafulla Dhariwal, Alex Nichol, Casey Chu, and Mark Chen. Hierarchical text-conditional image generation with clip latents. **2**
- [71] Aditya Ramesh, Mikhail Pavlov, Gabriel Goh, Scott Gray, Chelsea Voss, Alec Radford, Mark Chen, and Ilya Sutskever. Zero-shot text-to-image generation. *ICML*, Jul 2021.
- [72] Robin Rombach, Andreas Blattmann, Dominik Lorenz, Patrick Esser, and Björn Ommer. High-resolution image synthesis with latent diffusion models. In *CVPR*, pages 10684–10695, June 2022.
- [73] Chitwan Saharia, William Chan, Saurabh Saxena, Lala Li, Jay Whang, Emily Denton, Seyed Kamyar, Seyed Ghasemipour, Burcu Karagol, SSara Mahdavi, RaphaGontijo Lopes, Tim Salimans, Jonathan Ho, DavidJ Fleet, and Mohammad Norouzi. Photorealistic text-to-image diffusion models with deep language understanding. **2**
- [74] Christoph Schuhmann, Romain Beaumont, Richard Vencu, Cade Gordon, Ross Wightman, Mehdi Cherti, Theo Coombes, Aarush Katta, Clayton Mullis, Mitchell Wortsman, et al. Laion-5b: An open large-scale dataset for training next generation image-text models. *Advances in Neural Information Processing Systems*, 35:25278–25294, 2022. **4**
- [75] Christoph Schuhmann, Richard Vencu, Romain Beaumont, Robert Kaczmarczyk, Clayton Mullis, Aarush Katta, Theo Coombes, Jenia Jitsev, and Aran Komatsuzaki. Laion-400m: Open dataset of clip-filtered 400 million image-text pairs. *arXiv preprint arXiv:2111.02114*, 2021. **2, 4**
- [76] Dustin Schwenk, Apoorv Khandelwal, Christopher Clark, Kenneth Marino, and Roozbeh Mottaghi. A-okvqa: A benchmark for visual question answering using world knowledge. In *European Conference on Computer Vision*, pages 146–162. Springer, 2022. **4**
- [77] Wenqi Shao, Yutao Hu, Peng Gao, Meng Lei, Kaipeng Zhang, Fanqing Meng, Peng Xu, Siyuan Huang, Hongsheng Li, Yu Qiao, et al. Tiny l1vm-ehub: Early multimodal experiments with bard. *arXiv preprint arXiv:2308.03729*, 2023. **2**
- [78] Piyush Sharma, Nan Ding, Sebastian Goodman, and Radu Soricut. Conceptual captions: A cleaned, hypernymed, image alt-text dataset for automatic image captioning. In *Proceedings of the 56th Annual Meeting of the Association for Computational Linguistics (Volume 1: Long Papers)*, pages 2556–2565, 2018. **2, 4**
- [79] Oleksii Sidorov, Ronghang Hu, Marcus Rohrbach, and Amanpreet Singh. Textcaps: a dataset for image captioning with reading comprehension. In *Computer Vision—ECCV 2020: 16th European Conference, Glasgow, UK, August 23–28, 2020, Proceedings, Part II 16*, pages 742–758. Springer, 2020. **4**
- [80] Amanpreet Singh, Vivek Natarajan, Meet Shah, Yu Jiang, Xinlei Chen, Dhruv Batra, Devi Parikh, and Marcus Rohrbach. Towards vqa models that can read. In *Proceedings of the IEEE/CVF conference on computer vision and pattern recognition*, pages 8317–8326, 2019. **4**
- [81] Krishna Srinivasan, Karthik Raman, Jiecao Chen, Michael Bendersky, and Marc Najork. Wit: Wikipedia-based image text dataset for multimodal multilingual machine learning. In *Proceedings of the 44th International ACM SIGIR Conference on Research and Development in Information Retrieval*, pages 2443–2449, 2021. **14**
- [82] Quan Sun, Qiying Yu, Yufeng Cui, Fan Zhang, Xiaosong Zhang, Yueze Wang, Hongcheng Gao, Jingjing Liu, Tiejun Huang, and Xinlong Wang. Generative pretraining in multimodality. Jul 2023. **3**
- [83] Rohan Taori, Ishaan Gulrajani, Tianyi Zhang, Yann Dubois, Xuechen Li, Carlos Guestrin, Percy Liang, and Tatsunori B. Hashimoto. Stanford alpaca: An instruction-following llama model. [https://github.com/tatsu-lab/stanford\\_alpaca](https://github.com/tatsu-lab/stanford_alpaca), 2023. **3, 4**
- [84] InternLM Team. Internlm: A multilingual language model with progressively enhanced capabilities. <https://github.com/InternLM/InternLM>, 2023. **2, 3, 4, 8**
- [85] Hugo Touvron, Thibaut Lavril, Gautier Izacard, Xavier Martinet, Marie-Anne Lachaux, Timothée Lacroix, Baptiste Rozière, Naman Goyal, Eric Hambro, Faisal Azhar, et al. Llama: Open and efficient foundation language models. *arXiv.org*, 2023. **2, 3**
- [86] Hugo Touvron, Louis Martin, Kevin Stone, Peter Albert, Amjad Almahairi, Yasmine Babaei, Nikolay Bashlykov, Soumya Batra, Prajjwal Bhargava, Shruti Bhosale, et al. Llama 2: Open foundation and fine-tuned chat models, 2023. **2, 3, 8**
- [87] Ashish Vaswani, Noam Shazeer, Niki Parmar, Jakob Uszkoreit, Llion Jones, Aidan N Gomez, Lukasz Kaiser, and Illia Polosukhin. Attention is all you need. *Advances in Neural Information Processing Systems (NeurIPS)*, 30, 2017. **3**
- [88] Bin Wang, Fan Wu, Xiao Han, Jiahui Peng, Huaping Zhong, Pan Zhang, Xiaoyi Dong, Weijia Li, Wei Li, Jiaqi Wang, et al. Vigc: Visual instruction generation and correction. *arXiv.org*, 2023. **3, 4**
- [89] Weihang Wang, Qingsong Lv, Wenmeng Yu, Wenyi Hong, Ji Qi, Yan Wang, Junhui Ji, Zhuoyi Yang, Lei Zhao, Xixuan Song, Jiazheng Xu, Bin Xu, Juanzi Li, Yuxiao Dong, Ming Ding, and Jie Tang. Cogvlm: Visual expert for pretrained language models, 2023. **3**
- [90] Haoning Wu, Zicheng Zhang, Erli Zhang, Chaofeng Chen, Liang Liao, Annan Wang, Chunyi Li, Wenxiu Sun, Qiong Yan, Guangtao Zhai, et al. Q-bench: A benchmark for general-purpose foundation models on low-level vision. *arXiv preprint arXiv:2309.14181*, 2023. **2, 7**
- [91] Peng Xu, Wenqi Shao, Kaipeng Zhang, Peng Gao, Shuo Liu, Meng Lei, Fanqing Meng, Siyuan Huang, Yu Qiao, and Ping Luo. L1vm-ehub: A comprehensive evaluation benchmark for large vision-language models, 2023. **16**
- [92] An Yang, Junshu Pan, Junyang Lin, Rui Men, Yichang Zhang, Jingren Zhou, and Chang Zhou. Chinese clip: Contrastive vision-language pretraining in chinese. *arXiv.org*, 2022. **2, 3, 4**
- [93] Michihiro Yasunaga, Armen Aghajanyan, Weijia Shi, Richard James, Jure Leskovec, Percy Liang, Mike Lewis, Luke Zettlemoyer, and Wen-tau Yih. Retrieval-augmented multimodal language modeling. 2023. **3**
- [94] Qinghao Ye, Haiyang Xu, Guohai Xu, Jiabo Ye, Ming Yan, Yiyang Zhou, Junyang Wang, Anwen Hu, Pengcheng Shi, Yaya Shi, et al. mplug-owl: Modularization empowers

- large language models with multimodality. *arXiv.org*, 2023. 3, 6, 7
- [95] Shukang Yin, Chaoyou Fu, Sirui Zhao, Ke Li, Xing Sun, Tong Xu, and Enhong Chen. A survey on multimodal large language models. *arXiv preprint arXiv:2306.13549*, 2023. 2
- [96] Lili Yu, Bowen Shi, Ramakanth Pasunuru, Benjamin Muller, Olga Golovneva, Tianlu Wang, Arun Babu, Binh Tang, Brian Karrer, Shelly Sheynin, Candace Ross, Adam Polyak, Russell Howes, Vasu Sharma, Puxin Xu, Hovhannes Tamoyan, Oron Ashual, Uriel Singer, Shang-Wen Li, Susan Zhang, Gargi Ghosh, Yaniv Taigman, Maryam Fazel-Zarandi, Asli Celikyilmaz, Luke Zettlemoyer, and Armen Aghajanyan. Scaling autoregressive multi-modal models: Pretraining and instruction tuning. 3
- [97] Aohan Zeng, Xiao Liu, Zhengxiao Du, Zihan Wang, Hanyu Lai, Ming Ding, Zhuoyi Yang, Yifan Xu, Wendi Zheng, Xiao Xia, Weng Lam Tam, Zixuan Ma, Yufei Xue, Jidong Zhai, Wenguang Chen, Zhiyuan Liu, Peng Zhang, Yuxiao Dong, and Jie Tang. GLM-130b: An open bilingual pre-trained model. In *The Eleventh International Conference on Learning Representations (ICLR)*, 2023. 3
- [98] Yan Zeng, Hanbo Zhang, Jiani Zheng, Jiangnan Xia, Guoqiang Wei, Yang Wei, Yuchen Zhang, and Tao Kong. What matters in training a gpt4-style language model with multi-modal inputs? *ArXiv*, abs/2307.02469, 2023. 6, 17
- [99] Haotian Zhang, Pengchuan Zhang, Xiaowei Hu, Yen-Chun Chen, Liunian Li, Xiyang Dai, Lijuan Wang, Lu Yuan, Jenq-Neng Hwang, and Jianfeng Gao. Glipv2: Unifying localization and vision-language understanding. *Advances in Neural Information Processing Systems (NeurIPS)*, 35:36067–36080, 2022. 3
- [100] Susan Zhang, Stephen Roller, Naman Goyal, Mikel Artetxe, Moya Chen, Shuohui Chen, Christopher Dewan, Mona Diab, Xian Li, Xi Victoria Lin, et al. Opt: Open pre-trained transformer language models, 2022. *arXiv.org*. 3
- [101] Haozhe Zhao, Zefan Cai, Shuzheng Si, Xiaojian Ma, Kaikai An, Liang Chen, Zixuan Liu, Sheng Wang, Wenjuan Han, and Baobao Chang. Mmicl: Empowering vision-language model with multi-modal in-context learning. *arXiv.org*, 2023. 3, 6
- [102] Haozhe Zhao, Zefan Cai, Shuzheng Si, Xiaojian Ma, Kaikai An, Liang Chen, Zixuan Liu, Sheng Wang, Wenjuan Han, and Baobao Chang. Mmicl: Empowering vision-language model with multi-modal in-context learning. *ArXiv*, abs/2309.07915, 2023. 6
- [103] Zhiyuan Zhao, Linke Ouyang, Bin Wang, Siyuan Huang, Pan Zhang, Xiaoyi Dong, Jiaqi Wang, and Conghui He. Mllm-dataengine: An iterative refinement approach for mllm. *arXiv.org*, 2023. 3
- [104] Deyao Zhu, Jun Chen, Xiaoqian Shen, Xiang Li, and Mohamed Elhoseiny. Minigt-4: Enhancing vision-language understanding with advanced large language models. *arXiv.org*, 2023. 2, 3, 6, 7, 17
- [105] Wanrong Zhu, Jack Hessel, Anas Awadalla, Samir Yitzhak Gadre, Jesse Dodge, Alex Fang, Youngjae Yu, Ludwig Schmidt, William Yang Wang, and Yejin Choi. Multimodal c4: An open, billion-scale corpus of images interleaved

with text. *arXiv preprint arXiv:2304.06939*, 2023. 4

## A. Experiment Details

### A.1. Pre-training

The multi-modal pre-training process employs 1.1 billion images alongside 77.7 billion text tokens, including both public datasets and in-house concept data (Sec. B) collected from public websites, possessing over 11 million semantic concepts. The paired and interleaved text-image data includes 50.6 billion English text tokens and 17.1 billion Chinese text tokens. Furthermore, approximately 10 billion text tokens (5 billion English text and 5 billion Chinese text), sampled from the InternLM pre-training dataset [30], are incorporated to maintain the model’s linguistic proficiencies. Prior to the training process, all pre-training data underwent a thorough cleaning procedure to ensure its quality and reliability.

The optimization algorithm employed is AdamW, with hyperparameter settings as follows:  $\beta_1=0.9$ ,  $\beta_2=0.95$ ,  $eps=1e-8$ . The maximum learning rates for the perceive sampler and the large language model are configured at  $2e-4$  and  $4e-5$ , respectively, following a cosine learning rate schedule. The minimum learning rate is set at  $1e-5$ . Additionally, a linear warm-up is applied over the initial 200 steps. The training procedure employs a batch size of approximately 15.7 million tokens and spans 8,000 iterations. Utilizing such a large batch size in conjunction with a limited number of iterations contributes to stable training dynamics while also aiding in the preservation of LLM’s inherent capabilities. The overall multi-modal pre-training process requires 128 Nvidia A100 GPUs for around 80 hours.

### A.2. Supervised Fine-tuning

We adopt the Low-Rank Adaption (LoRA) [31] for the supervised fine-tuning process, which is composed of a *Multi-task Training* phase and a *Instruction Tuning* phase. The perceive sampler is concurrently trained, albeit with a distinct learning rate. Specifically, LoRA is applied to both the attention layer and the feed-forward network (FFN). We find that a high LoRA rank is conducive to imbuing the model with new capabilities; consequently, we set the LoRA rank and alpha parameter both to 256. The model is trained using a global batch size of 256 over 18,000 iterations in *Multi-task Training* phase. The learning rates are set to  $5e^{-5}$  for the LoRA layer and  $2e^{-5}$  for the perceive sampler.

For the *Instruction Tuning* phase, we maintain a batch size of 256 and execute the tuning over 1000 iterations with a small learning rate  $1e^{-5}$ .

## B. Concept Data

As illustrated by Figure A4 and Figure A5, our concept dataset is curated from Wikipedia<sup>3</sup> and Baidu Baike<sup>4</sup>, comprising 2 million English vision-language concepts and 9 million Chinese vision-language concepts. Each concept consists of an image paired with corresponding descriptions. Examples are illustrated in Figure A6 and Figure A7. In comparison to the WIT [81] dataset, which comprises approximately 2 million multimodal English and Chinese concepts after removing expired links and noisy samples, our multimodal concept data significantly surpasses it in terms of data volume and diversity.

**Experimental results.** Here, we study the effectiveness of the concept dataset on our framework with three settings: 1) remove our In-house Concept data. 2) replace our In-house Concept data with the WIT [81] dataset. 3) the default pre-training setting. As results shown in Table A13, compared to the baseline, the WIT improves the model performance on both English and Chinese benchmarks. Further, when using our larger and more diverse In-house Concept dataset, the model surpasses the WIT baseline by a large margin on both benchmarks, especially on the Chinese knowledge-based benchmark CCBench.

## C. Interleaved Image-Text Composition

### C.1. Format Details

**Text Generation.** As the interleaved image-text dataset is collected from public websites, the acquired dataset contains noise, particularly in the form of marketing and advertising content. To address this, We utilize GPT-4 to assess whether an individual sentence contains noise and identify the type of noise, which includes advertisement, reference, and recommendations (e.g., *external articles/answers*). Any sentences identified as noisy are removed, and articles containing more than 30% noisy sentences are filtered out directly. After the cleaning, we formulate the training data in the following manner:

```
<|User|> : Write an illustrated article based on the
              given instruction: {Instruction} <eou>
<|Bot|> : [para1] ... [paraN] <eob>
```

Here,  $\{Instruction\}$  serves as a placeholder for the article-crafted instruction, such as a simple title, or a draft outline, etc. The  $[para_1]$  and  $[para_N]$  denote the first and last paragraphs, respectively.

**Image Spotting and Captioning.** In practice, we formulate the spotting and captioning task with the following format:

<sup>3</sup><https://www.wikipedia.org/>

<sup>4</sup><https://baike.baidu.com/>

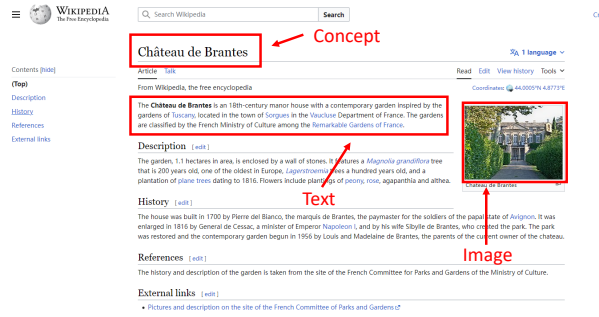


Figure A4. Extract vision-language concepts from Wikipedia.



Figure A5. Extract vision-language concepts from Baidu Baike.

Concept-specific Data	MMBench	CCBench
-	72.9	44.0
WIT (2M)	73.5	45.1
In-house Concept data (11M)	74.4	47.6

Table A13. Ablation of the concept-specific data used in the pre-training phase.

$\langle |User| \rangle : [seg_1][para_1] \dots [seg_N][para_N]$  *Based on the above text, select the appropriate locations for inserting images and give the image captions*  $\langle eou \rangle$

$\langle |Bot| \rangle : I$  think images can be added under the  $\{x_1\}, \dots, \{x_k\}$  paragraphs. The image captions are as follows:  $\{x_1\}$  paragraph:  $\{cap_1\}, \dots, \{x_k\}$  paragraph:  $\{cap_k\}$   $\langle eob \rangle$

Here,  $[seg_1]$  serves as an index token to pinpoint the specific paragraph index. The placeholders  $\{x_1\}$  and  $\{x_k\}$  represent the positions for the first and last image locations, respectively. Correspondingly,  $\{cap_1\}$  and  $\{cap_k\}$  act as the generated captions associated with those image locations.

**Image Retrieval and Selection.** The training data is struc-

ured in the following manner:

$\langle |User| \rangle : [para_1] \dots [para_i][img_i][para_{i+1}] \dots [para_j]$   
*Based on the given context and candidate images, select the appropriate image.*  
*Candidate images include:* $[img_j^1] \dots [img_j^m]$   
 $\langle eou \rangle$   
 $\langle |Bot| \rangle : The \{selected\ index\} image. \langle eob \rangle$

In this configuration,  $[img_i]$  denotes the image associated with the  $i^{th}$  paragraph. The terms  $[img_j^1], \dots, [img_j^m]$  represent the candidate images retrieved by CLIP [67] based on  $\{cap_1\}, \dots, \{cap_k\}$  from an image pool. Meanwhile,  $\{selected\ index\}$  acts as a placeholder indicating the index of the final selected image.

## C.2. Image-Text Composition Evaluation Details

**Grading Criteria.** Due to the lack of existing metrics to evaluate the interleaved image-text article quality, we designed a detailed user study metric, including eight dimensions: four text-related dimensions (instruction following, writing quality, logic, factualness), three image-related dimensions (image-text consistency, image informative, image consistency), and one subjective preference. Each dimension contains three levels of score: Excellent (5 points), Medium (3 points), and Poor (1 point).

With a given topic, the human expert and GPT4-V are asked to grade the articles generated by different models (in a double-blind manner) in each of the eight dimensions. Specifically, for each time of scoring one article, the points of four text-related dimensions are summarized and divided by the full score of text (20 points) into a text-related score, and the three image-related dimensions are summarized and divided by the full score of image (15 points) into an image-related score. The subjective preference is divided by five into a subjective preference score. The average score, which is the average number of the text-related score, the image-related score, and the subjective preference score, is taken as the overall result for a human expert or the GPT4-V. The scores of 10 human experts are averaged for the final human evaluation result. The GPT4-V assessments are performed three times to calculate the average GPT4-V score.

**Details of Eight Evaluation Dimensions.** The details of each of the eight dimensions are as follows:

1) *Instruction following* evaluate the content based on the degree of task completion, and evaluate whether the generated article conforms to the given topic and meets the style required by the topic (such as meeting the specified title, complying with the given abstract, keywords, outline, etc.).

Scoring Levels:

1 point: Severely non-compliant with instructions;

3 points: Basically compliant with instructions;

---

### GPT4-Vision Evaluation Prompt

---

There is an interleaved text-image article that should follow the instruction:  
{*Instruction*}  
The article’s content:  
{*Article content*}  
Based on the given instruction and article, please evaluate this article by answering the following questions:  
Please evaluate whether the article meets the requirements and choose the score from the given scoring level in each question:  
Q1: {*Q1*}  
...  
Q8: {*Q8*}  
Please give a rating for each question one by one and explain the reason.  
The output format should be:  
”Final Score:  
Q1: (1 or 3 or 5) points, Reason: xxx  
...  
Q8: (1 or 3 or 5) points, Reason: xxx ”

---

Table A14. The prompt used for GPT4-V evaluation. {*Instruction*}, {*Article content*}, and {*Q1*}...{*Q8*} will be replaced by the instruction, the interleaved image-text article, and explanations and scoring levels of eight dimensions, respectively.

5 points: Highly compliant with instructions.

2) *Writing quality* evaluate the language quality based on the content of the article (including but not limited to vocabulary, grammar, word choice and sentence making, etc.). It requires accurate word expression, rich language, and correct grammar. Scoring Levels:

- 1 point: Poor;
- 3 points: Medium;
- 5 points: Excellent.

3) *Logic* evaluate the article based on the logical rationality of the content (the content of the article should try to follow the common rules in daily life, have clear cause and effect relationships, and have no obvious logical fallacies, etc.). Scoring Levels:

- 1 point: Severe logical errors (3 or more instances);
- 3 points: Minor logical errors (1-3 instances);
- 5 points: Clear logic and explicit cause-and-effect relationship.

4) *Factualness* evaluate the article based on the accuracy of the content (the content of the article should be as consistent as possible with common sense of life and scientific knowledge, without illusions or fabricated facts, and the use of relevant documents and materials should be reasonable and appropriate). Scoring Levels:

- 1 point: Severe factual errors or delusions (3 or more instances);
- 3 points: Minor factual errors or delusions (1-3 instances);
- 5 points: Factually correct, with no obvious delusions or fabrications.

5) *Image-text consistency* evaluate the relevance of the images to the topic of the article. Scoring Levels:

1 point: The illustration is unrelated to the article’s theme;

3 points: The illustration is related to the article’s theme, but not closely;

5 points: The illustration is closely related to the article’s theme.

6) *Image informative* evaluate the relevance of the main content of the accompanying images and related paragraphs, and the informativeness of the images. Scoring Levels:

- 1 point: The illustration is completely uninformative;
- 3 points: The illustration is related to the main content of the relevant paragraph;

5 points: In addition to the above, the illustration also conveys extra supplementary information not present in the article.

7) *Image consistency* evaluate the subject consistency between the accompanying pictures (for instance, when writing about my cat, the accompanying image should ideally be of the same cat.). Scoring Levels:

- 1 point: The subjects in some illustrations differ greatly;
- 3 points: The subjects in some illustrations appear similar, but upon closer examination, differences exist;
- 5 points: Completely satisfies image consistency.

8) *Subjective preference* is an overall subjective score about the quality of the generated article. Scoring Levels:

- 1 point: Poor;
- 3 points: Medium;
- 5 points: Excellent.

**GPT4-V Evaluation.** Besides human experts, we leverage GPT4-V api, which can take interleaved text-image articles as inputs for evaluation. The input prompt format is shown in Table A14. {*Instruction*}, {*Article content*} will be replaced by the requirements of the article and the composed interleaved image-text article during evaluation, respectively. {*Q1*}...{*Q8*} indicates the explanations and scoring levels of eight dimensions as in **Details of Eight Evaluation Dimensions**, e.g., ”Instruction following evaluate the content ... Scoring Levels: ...”. We manually check the output of the GPT4-V api to collect the final score.

## D. More Benchmark results.

**Tiny LVLM [91]** is an ability-level benchmark, which evaluates the MLLM performance from five different abilities. We report the results in Table A15. Our InternLM-Xcomposer-VL gets the best overall results and the Top-3 performance in most abilities, even surpassing a commercial MLLM, i.e., Google Bard.

---

<sup>5</sup><https://bard.google.com/>.

Refer to Tiny LVLM at [https://github.com/OpenGVLab/Multi-Modality-Arena/tree/main/tiny\\_lvlm\\_evaluation](https://github.com/OpenGVLab/Multi-Modality-Arena/tree/main/tiny_lvlm_evaluation)



Method	Overall	VR	VP	VKA	VC	OH
MiniGPT-4 [104]	192.6	37.6	37.8	17.6	49.0	50.7
LLaVA [50]	197.0	41.6	38.3	18.7	49.4	49.0
VisualGLM [24]	211.9	37.3	36.3	46.9	37.6	54.0
Otter [41]	216.4	41.6	37.0	15.1	52.4	74.0
LLaMA-A-V2 [27]	229.2	43.5	46.8	22.3	56.0	60.7
Lynx [98]	279.2	52.2	<u>65.8</u>	17.6	57.4	86.3
BLIP2 [42]	284.7	44.9	49.0	<u>64.1</u>	44.0	82.7
InstructBLIP [18]	300.6	46.7	48.0	61.7	<u>59.2</u>	85.0
LLaVA-1.5 [49]	307.2	55.6	49.0	57.0	57.2	<u>88.3</u>
Qwen-VL-Chat [4]	316.8	<u>62.4</u>	<u>54.5</u>	55.1	54.8	<u>90.0</u>
Bard <sup>5</sup>	319.6	<u>64.2</u>	<u>57.0</u>	<u>68.1</u>	<u>59.6</u>	70.7
Ours	<b>322.5</b>	<u>55.8</u>	53.8	<u>64.1</u>	<u>61.8</u>	<u>87.0</u>

Table A15. **Evaluation of Tiny LVLM test set.** Here we report all the sub-tasks, including visual reasoning (VR), visual perception (VP), visual knowledge acquisition (VKA), visual commonsense (VC), and object hallucination (OH).

## E. More Qualitative Results.

Figure A8-A13 shows some interleaved image-text compositions generated by InternLM-XComposer. Figure A14 and Figure A15 give some conversation cases when chatting with InternLM-XComposer. Our model exhibits an excellent ability in multilingual interleaved composition and conversation.



### ***Château de Brantes***

The Château de Brantes is an 18th-century manor house with a contemporary garden inspired by the gardens of Tuscany, located in the town of Sorgues in the Vaucluse Department of France. The gardens are classified by the French Ministry of Culture among the Remarkable Gardens of France.



### ***POP tennis***

POP tennis (originally known as paddle tennis) is a racket sport adapted from tennis and played for over a century. Compared to tennis, the court is smaller, has no doubles lanes, and the net is lower. Paddle tennis is played with a solid perforated paddle, as opposed to a strung racquet, and a lower pressure tennis ball. The same court is used for both singles and doubles, with doubles being the dominant form of play. The smaller court size adds a strong emphasis and advantage to net play and creates a fast and reaction-based game. Growing in popularity, local leagues and tournaments can be found worldwide.



### ***Alluvial plain***

An alluvial plain is a largely flat landform created by the deposition of sediment over a long period of time by one or more rivers coming from highland regions, from which alluvial soil forms. A floodplain is part of the process, being the smaller area over which the rivers flood at a particular period of time, whereas the alluvial plain is the larger area representing the region over which the floodplains have shifted over geological time.



### ***Aeronca Champion***

The Aeronca Model 7 Champion, commonly known as the "Champ", or "Airknocker", is a single-engine light airplane with a high wing, generally configured with fixed conventional landing gear and tandem seating for two occupants.



### ***Tijuana River***

The Tijuana River (Spanish: Río Tijuana) is an intermittent river, 120 mi (195 km) long, near the Pacific coast of northern Baja California state in northwestern Mexico and Southern California in the western United States. The river is heavily polluted with raw sewage from the city of Tijuana, Mexico.



### ***Ficus microcarpa***

*Ficus microcarpa*, also known as Chinese banyan, Malayan banyan, Indian laurel, curtain fig, or gajumaru (ガジュマル), is a tree in the fig family Moraceae. It is native in a range from China through tropical Asia and the Caroline Islands to Australia. It is widely planted as a shade tree and frequently misidentified as *F. retusa* or as *F. nitida* (syn. *F. benjamina*)



### ***The Flintstone Kids***

The Flintstone Kids is an American animated television series produced by Hanna-Barbera. It is an alternative incarnation of the studio's original animated series The Flintstones. The series depicts juvenile versions of the main characters from the original show. It aired from September 13, 1986, to November 14, 1987, on ABC. Unlike the previous shows, this was the first Flintstone series not to have a laugh track.

Figure A6. Examples from our vision-language concept dataset.



### 雷暴

雷暴 (thunderstorms), 是热带和温带地区可见的局地性强对流天气。雷暴发生时可伴随有雷击、闪电、强风和强降水, 例如雨或冰雹。雷暴可发生于春季和夏季, 常见的例子是夏季午后, 但也可能在冬季随暴风雪发生, 被称为雷雪 (thundersnow)。



### 对联

对联, 又称对偶、门对、春贴、春联、对子、楹联等, 是写在纸、布上或刻在竹子、木头、柱子上的对偶语句。对联对仗工整, 平仄协调, 是一字一音的汉语独特的艺术形式。对联是中国传统文化瑰宝。



### 兵马俑

兵马俑, 即秦始皇陵兵马俑, 亦简称秦兵马俑或秦俑, 是第一批全国重点文物保护单位、第一批中国世界遗产, 位于今陕西省西安市临潼区秦始皇陵以东1.5千米处的兵马俑坑内。



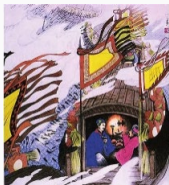
### 乐山大佛

乐山大佛 (Leshan Giant Buddha), 又名凌云大佛, 全称为“嘉州凌云寺大弥勒石像”, 位于四川省乐山市南岷江东岸凌云寺侧, 濒大渡河、青衣江和岷江三江汇流处。大佛为弥勒佛坐像, 通高71米, 是中国最大的一尊摩崖石刻造像。乐山大佛开凿于唐代开元元年 (713年), 完成于贞元十九年 (803年), 历时约九十年。



### 金门大桥

金门大桥 (Golden Gate Bridge), 又称“金门海峡大桥”, 是美国境内连接旧金山市区和北部的马林郡的跨海通道, 位于金门海峡之上, 是美国旧金山的主要象征。



### 草船借箭

草船借箭是中国古典名著《三国演义》中赤壁之战的一个故事。借箭由周瑜故意提出 (限十天内造十万支箭), 机智的诸葛亮一眼识破是一条害人计, 却淡定表示“只需要三天”。后来, 有鲁肃帮忙, 诸葛亮再利用曹操多疑的性格, 调了二十条草船诱敌, 终于“借”到了十余支箭。



### 青之岛

青之岛 (日语: 青ヶ島, 英语: Aogashima) 是日本伊豆群岛南部一座火山岛, 是伊豆群岛中有人居住的最南端的岛屿, 行政上属于日本东京都八丈支厅青岛村管辖。

Figure A7. Examples from our vision-language concept dataset.

## Write a travel guide titled “Shanghai Travel Guide”.

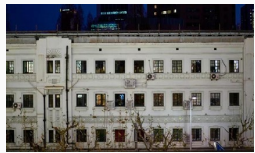
### Shanghai Travel Guide

Shanghai is the largest city in China and one of the most populous cities in the world, with a population of over 24 million people. The city is known for its modern skyscrapers, bustling financial district, and vibrant nightlife. Shanghai is also home to some of the country's top tourist attractions, including the Bund, Yuyuan Garden, and the Oriental Pearl Tower. In this guide, we'll provide you with all the information you need to plan your trip to Shanghai, including tips on where to stay, what to do, and how to get around.



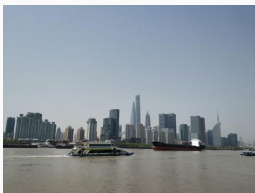
#### Where to Stay in Shanghai

When it comes to finding a place to stay in Shanghai, there are plenty of options to choose from. If you're looking for a luxury experience, consider staying at one of the city's five-star hotels, such as the Fairmont Peace Hotel or the Waldorf Astoria Shanghai on the Bund. These hotels offer stunning views of the city skyline, luxurious amenities, and impeccable service.



If you're looking for something more budget-friendly, there are plenty of hostels and guesthouses throughout the city that offer affordable accommodations. Some popular areas to stay include the Xintiandi neighborhood, which is known for its trendy bars and restaurants, and the French Concession, which is filled with charming cafes and boutiques.

#### What to Do in Shanghai



One of the best ways to explore Shanghai is by taking a stroll along the Bund, a waterfront promenade that offers stunning views of the city skyline. You can also visit the Yu Garden, a traditional Chinese garden that dates back to the Ming Dynasty, and the Shanghai Museum, which houses an impressive collection of Chinese art and artifacts.

Another popular attraction in Shanghai is the Oriental Pearl Tower, a television tower that offers panoramic views of the city. You can also take a boat ride on the Huangpu River, which runs through the heart of the city, and visit the Jade Buddha Temple, a Buddhist temple that houses two jade Buddha statues.



#### How to Get Around in Shanghai

The best way to get around Shanghai is by using public transportation, which includes buses, subways, and taxis. The city's subway system is extensive and easy to use, with stations located throughout the city. Buses are also a convenient way to get around, although they can be crowded during rush hour.



Taxis are available throughout the city, but make sure to agree on a price before getting into the taxi so you don't get ripped off. Another option is to rent a bicycle or scooter, which will allow you to explore the city at your own pace.

#### Tips for Visiting Shanghai



1. Dress appropriately: Shanghai is a conservative city, so it's important to dress modestly when visiting temples and other religious sites. Cover your shoulders and knees, and avoid wearing revealing clothing.

2. Learn some basic Mandarin: While many people in Shanghai speak English, it's always helpful to know some basic Mandarin phrases, such as "hello," "thank you," and "excuse me."



3. Be aware of pickpockets: Like any major city, Shanghai has its fair share of pickpockets. Keep your valuables close to you and be vigilant about your surroundings.

...

In conclusion, Shanghai is a vibrant and exciting city that offers something for everyone. Whether you're interested in history, culture, or just want to have a good time, Shanghai has it all. With its towering skyscrapers, bustling streets, and rich cultural heritage, Shanghai is a must-visit destination for anyone traveling to China.



Figure A8. Interleaved composition generated by InternLM-XComposer.

## 以“又见敦煌”为题写一篇旅游攻略。

### 又见敦煌

敦煌，位于甘肃省西北部，地处河西走廊西端，是古代丝绸之路上的重要交通枢纽和商埠重镇。它拥有着丰富的历史文化遗产，包括莫高窟、鸣沙山月牙泉、雅丹魔鬼城等著名景点。同时，敦煌也是中国历史文化名城之一，有着深厚的文化底蕴和独特的民俗风情。



#### 一、莫高窟

莫高窟，又名“千佛洞”，是中国四大石窟之一，始建于十六国的前秦时期，距今已有1600多年的历史。它是世界上现存规模最大、内容最丰富的佛教艺术宝库，被誉为“东方卢浮宫”。莫高窟内共有735个洞窟，壁画总面积达45000多平方米，彩塑佛像5000余尊，是世界上最大的佛教艺术中心之一。在这里，游客可以欣赏到精美的壁画、雕塑和音乐表演，感受佛教文化的博大精深。



#### 二、鸣沙山月牙泉

鸣沙山月牙泉是一处自然奇观，位于敦煌市西北约40公里处的沙漠中。这里地势平坦，沙丘连绵起伏，形成了一片广袤无垠的沙漠景观。而月牙泉则静静地镶嵌在这片沙漠之中，泉水清澈见底，形状如新月，故称“月牙泉”。每到夜晚，月亮升起时，月牙泉周围会发出阵阵清脆的响声，犹如天籁之音，令人心旷神怡。



#### 三、雅丹魔鬼城

雅丹魔鬼城是一座典型的风蚀地貌，位于敦煌市西南约100公里的戈壁滩上。这里的地貌奇特，呈现出一种荒凉、神秘、恐怖的景象。由于长期受到风吹日晒雨淋，这里的岩石表面已经变得凹凸不平，形成了各种形态各异的造型，有的像动物，有的像人物，有的像建筑，让人不禁感叹大自然的鬼斧神工。



#### 四、其他景点

除了莫高窟、鸣沙山月牙泉和雅丹魔鬼城之外，敦煌还有许多其他值得一游的景点，如玉门关、阳关、锁阳城、汉长城遗址等。这些景点都具有悠久的历史和文化价值，吸引着众多游客前来参观游览。



#### 五、特色美食

敦煌的特色美食也非常丰富，其中最著名的当属驴肉黄面了。驴肉黄面是一道以驴肉为主要食材的面食，味道鲜香可口，深受当地人和游客的喜爱。此外，还有羊肉泡馍、胡羊焖饼、烤全羊等特色美食，都是不容错过的美味佳肴。



#### 六、旅游小贴士

1. 敦煌气候干燥，日照强烈，紫外线较强，建议游客做好防晒措施，携带防晒霜、遮阳帽、太阳镜等物品。2. 敦煌属于高原地区，海拔较高，游客应注意休息，避免剧烈运动，以免出现高原反应。3. 敦煌旅游景点较多，游客应提前规划好行程，合理安排时间，避免走马观花，错过重要的景点。4. 在敦煌旅游期间，要注意保护环境，不乱扔垃圾，不破坏文物古迹，做一个文明的游客。总之，敦煌是一座历史悠久、文化底蕴深厚、风景优美的城市，是一个值得一游的好去处。希望这篇文章能够帮助您更好地了解敦煌，为您的旅行提供一些有用的信息。

Figure A9. Interleaved composition generated by InternLM-XComposer.

Write an article introducing World War 2 with the title “The World War 2”.

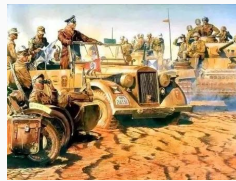
### The World War 2

World War II (WWII or WW2), also known as the Second World War, was a global war that lasted from 1939 to 1945. It involved the vast majority of the world's countries—including all of the great powers—eventually forming two opposing military alliances: the Allies and the Axis.



It was the most widespread war in history, with some 100 million military personnel, including 60 million on the Allied side and 30 million on the Axis side, participating in more than 5,000 air battles, land battles, and naval engagements in 60 countries across five continents.

On September 1, 1939, Germany invaded Poland, marking the start of Operation Barbarossa, the German invasion of the Soviet Union. On December 7, 1941, Japan launched a surprise attack on Pearl Harbor, Hawaii, resulting in the United States' entry into the war on the side of the Allies.



In June 1941, Nazi Germany invaded the Soviet Union during Operation Barbarossa. This marked the beginning of the largest tank battle in history, the Battle of Kursk, which took place between July 12 and August 23, 1943. The Soviets were able to inflict heavy losses on the Germans, forcing them to retreat back to their original positions.

The Battle of Stalingrad, which took place between August 1942 and February 1943, was one of the bloodiest battles in human history. During this time, the Red Army suffered an estimated 900,000 casualties, while the Wehrmacht lost approximately 600,000 soldiers.



The Battle of El Alamein, which took place between October 1942 and November 1943, was another major turning point in the war. Here, the British Eighth Army under General Bernard Montgomery defeated the German Afrika Korps led by Field Marshal Erwin Rommel at the Sidi Rezegh Pass near Tobruk, Libya.

This victory allowed the Allies to gain control of much of North Africa and paved the way for the eventual defeat of Adolf Hitler's forces in Europe.



The Battle of Midway, which took place between June 4-7, 1942, saw the U.S. Navy decisively defeat the Imperial Japanese Navy off the coast of Midway Atoll in the Pacific Ocean. This victory helped turn the tide of the war in favor of the Allies.

The Battle of Normandy, which took place between June 6-July 29, 1944, was the largest amphibious invasion in history. Over 160,000 Allied troops landed on the beaches of Normandy, France, supported by over 10,000 aircraft and nearly 5,000 landing craft.



After several weeks of fierce fighting, the Allies had secured a foothold in France and were able to begin advancing towards Germany.

The Battle of the Bulge, which took place between December 16, 1944, and January 25, 1945, was a last-ditch attempt by the German army to break through the Allied lines and end the war before it could be officially declared.



Despite being outnumbered and outgunned, the Allies were able to repel the German offensive and continue their advance towards Germany.

The Battle of Okinawa, which took place between April 1-May 22, 1945, was the final major battle of the Pacific Theater of World War II.



Here, the U.S. Marine Corps and the Ryukyu Islands Defense Force fought against the Imperial Japanese Army until the latter surrendered unconditionally on August 14, 1945.

The atomic bombings of Hiroshima and Nagasaki, which took place on August 6 and August 9, 1945, respectively, marked the first use of nuclear weapons in warfare.



These bombings resulted in the immediate deaths of tens of thousands of people and contributed to the rapid conclusion of the war.

Overall, World War II is remembered as one of the deadliest conflicts in human history, claiming the lives of millions of men, women, and children around the world.

Figure A10. Interleaved composition generated by InternLM-XComposer.

## 以“C919宣传广告”写一篇宣传广告。

### C919宣传广告

C919大型客机是中国自行研制、具有自主知识产权的大型喷气式民用飞机，座级158-168人，航程4075-5555公里。2017年5月14日，国产大飞机C919在上海浦东国际机场首飞成功！这是中国航空工业发展史上的一个重要里程碑，标志着我国成为继美国、俄罗斯之后世界上第三个能够设计制造大型客机的国家。



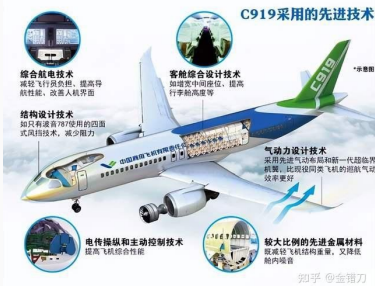
#### 1. C919的研发历程

1999年12月22日，国务院正式批准了中国商用飞机有限责任公司（COMAC）筹建；2002年6月29日，中俄两国政府在北京签署了关于联合研制和生产新型干线宽体客机的合作意向书；2003年9月25日，在人民大会堂举行了隆重的签字仪式；



2010年4月26日，第一架C919原型机在中国上海总装下线并进行了首次地面滑行试车（即“一地两检”）；同年11月30日，第二架C919完成全机静力试验并获得型号合格证（TC）；2018年02月28日，第三架C919顺利通过适航取证审定试飞并在北京首都机场着陆后转场至西安阎良进行交付前的系统调试与性能优化工作。

#### 2. C919的主要特点



**安全性高：**由于采用了先进的设计理念和技术手段，使得该机型具有良好的抗坠毁性以及超强的防冰雨雪能力等优点；此外它还配备了先进的电子飞行仪表系统和自动驾驶仪以提高飞行员操作效率降低人为因素对飞行安全造成影响等等一系列措施都为保证乘客生命财产安全提供了有力保障！

**舒适性好：**为了满足不同层次旅客需求而专门开发出符合人体工程学原理设计的经济舱座椅不仅美观大方而且坐起

来也非常舒服哦！另外还有宽敞明亮且视野开阔的全景式舷窗可以随时欣赏到窗外美丽景色呢~总之一句话概括就是两个字——高大上啊哈哈^\_^!!

**节能环保：**作为一款绿色出行交通工具当然不能落后于时代潮流啦对吧？所以设计师们在设计之初就充分考虑到了这一点并将其融入了整个机身结构当中从而大大降低了燃油消耗量同时还能有效减少尾气排放污染环境保护我们赖以生存的大好河山哟o(\*▽\*)o!! 以上便是小编为大家整理出来的全部内容希望对您有所帮助如果您还有其他疑问或者想了解更多相关资讯请继续关注本号后续推送文章敬请期待吧~(o▽o)/(^\_^)-☆

## 以“星链新闻稿”写一篇新闻稿。

### 星链新闻稿

北京时间2021年9月13日，星链（Starlink）在美国内华达州拉斯维加斯举行的第52届国际消费电子展（CES 2021）上展示了其卫星互联网服务。



在展会现场，SpaceX公司首席执行官埃隆·马斯克（Elon Musk）向与会者介绍了星链的最新进展和计划。他表示，星链将为全球提供高速、低延迟的网络接入服务，并将在未来几年内覆盖全球大部分地区。

据介绍，星链是一个由近1.2万颗通信卫星组成的系统，这些卫星分布在多个轨道上，以实现全球覆盖。目前，星链已经发射了约1900颗卫星，预计到2025年将达到4.2万颗。



对于用户来说，星链提供了高速、低延迟的网络接入服务，能够满足各种应用场景的需求。同时，星链还支持多终端设备接入，包括智能手机、平板电脑、笔记本电脑等。此外，星链还提供了一系列的增值服务，如视频点播、游戏加速等。

据了解，星链的服务价格相对较低，每月只需支付99美元即可享受高速、低延迟的网络接入服务。这对于那些生活在偏远地区或无法获得传统电信运营商服务的用户来说，无疑是一个福音。

RECHARGE	\$10	\$15	\$20	\$30	\$40	\$50	\$70	\$100
Rate	Light up to 15 days	Light up to 15 days	Light up to 23 days	Light up to 33 days	Light up to 40 days	Light up to 50 days	Light up to 70 days	Light up to 100 days

不过，也有一些人对星链的安全性提出了质疑。他们认为，星链可能会成为黑客攻击的目标，从而威胁用户的隐私和安全。对此，马斯克表示，星链采用了多种安全措施，包括加密算法、多重身份验证等，以确保用户的数据安全。

总的来说，星链是一项非常有前景的技术，它有望为全球用户提供高速、低延迟的网络接入服务。随着技术的不断发展和完善，相信星链将会为人类社会带来更多的便利和改变。

Figure A11. Interleaved composition generated by InternLM-XComposer.

Write an article about London travel guidance. First introduce the Must-See Attractions, then give some advices about the cultural experiences, then give some ideas about the Accommodation and Transportation, at last give a conclusion

London is one of the most popular travel destinations in the world, and for good reason. From its iconic landmarks to its rich history and vibrant culture, there is something for everyone in this bustling city. In this article, we will provide you with a comprehensive guide to help you make the most of your trip to London.



First, let's talk about the must-see attractions. London is home to some of the most famous landmarks in the world, including Buckingham Palace, the Tower of London, and Big Ben and the Houses of Parliament. If you're interested in history, be sure to visit the British Museum and the Tower of London, which is home to the Crown Jewels. For a more modern experience, check out the Shard, a skyscraper that offers stunning views of the city.

Next, let's talk about cultural experiences. London is known for its diverse and vibrant culture, and there are many ways to immerse yourself in it. If you're interested in theater, be sure to catch a show at the West End, which is home to some of the best theater in the world. If you're more interested in art, be sure to visit the Tate Modern and the National Gallery, which are home to some of the most famous works of art in the world.



Now, let's talk about accommodation. London has a wide range of accommodations to choose from, from luxury hotels to budget-friendly hostels. If you're looking for a luxury experience, be sure to check out the Shangri-La at the Shard, which offers stunning views of the city from its rooftop terrace. If you're on a budget, be sure to check out the YHA London St Pancras, which offers affordable accommodations in a central location.



Finally, let's talk about transportation. London has an extensive public transportation system, including the Tube, buses, and trams. If you're planning on using public transportation, be sure to purchase an Oyster card, which allows you to pay for your fares as you go. If you're planning on driving, be sure to check out the congestion charge, which is a fee that drivers must pay to enter central London during certain hours.

In conclusion, London is a city that has something for everyone. From its iconic landmarks to its rich history and vibrant culture, there is no shortage of things to see and do in this bustling city. With our comprehensive guide, you'll be able to make the most of your trip to London and create memories that will last a lifetime.

Figure A12. Interleaved composition generated by InternLM-XComposer.



撰写一篇关于318自驾的文章。 以下是大纲：  
开头介绍旅游原因。

接下来介绍旅游日程：

Day 1: 成都 - 雅安 - 泸定 - 磨西古镇

Day 2: 海螺沟 - 康定 - 新都桥

Day 3: 新都桥 - 雅江 - 理塘 - 稻城亚丁

最后总结旅游感受。

2019年8月，我们一家三口从成都出发，自驾前往稻城亚丁。

## 一、旅游原因



这次去稻城亚丁是临时起意，没有做任何攻略，只是在网上看了一些别人的游记，大概了解了一下景点分布和大致的游玩路线。因为之前去过九寨沟，所以对川西的美景非常向往，再加上孩子一直嚷嚷着要去观海沟的大冰瀑布，所以就有了这次说走就走的旅行。

## 二、旅游日程

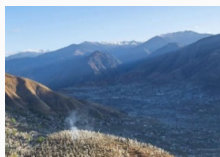


### Day 1: 成都 - 雅安 - 泸定 - 磨西古镇

早上八点从成都出发，第一站到达雅安，在雅安吃了午饭，然后驱车前往泸定桥。泸定桥位于四川省甘孜藏族自治州泸定县境内，横跨大渡河上，距今已有1700多年的历史。泸定桥始建于公元618年，原名铁索桥，又称飞夺泸定桥。1935年5月28日，中国工农红军红四方面军强渡大渡河，取得了“飞夺泸定桥”这一战役的重大胜利。泸定桥全长103米，宽2.7米，由13根铁链组成，每根铁链间距0.3米，共有铁锁260余个，每个铁锁重达200多公斤。当年红军战士们就是依靠这13根铁链与敌人展开殊死搏斗，最终取得了胜利。现在泸定桥已经修葺一新，供游客参观游览。

离开泸定桥后，我们继续赶路，大约下午五点左右到达磨西古镇。磨西古镇位于四川省甘孜藏族自治州泸定县内，距离康定市区约60公里，海拔2400米。磨西古镇建于明末清初，至今已有400多年的历史。这里曾经是古丝绸之路上的重要驿站，也是茶马古道的必经之地。如今，磨西古镇保存了大量的明清时期的建筑，包括寺庙、民居、商铺等，具有很高的历史文化价值。此外，磨西古镇还有著名的海螺沟景区，海螺沟位于四川省甘孜藏族自治州南部，地处青藏高原东缘，平均海拔4000米以上，被誉为“世界级冰川奇观”。我们在磨西古镇住了一晚，第二天的行程是从磨西古镇出发，前往海螺沟景区。

### Day 2: 海螺沟 - 康定 - 新都桥



第二天一大早，我们从磨西古镇出发，前往海螺沟景区。海螺沟位于

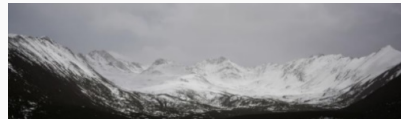
四川省甘孜藏族自治州南部的贡嘎山北坡，距离磨西古镇约80公里。海螺沟是中国国家AAAAA级风景名胜区，也是世界自然遗产——四川大熊猫栖息地的组成部分之一。海螺沟拥有壮丽的山峰、清澈的溪流、茂密的原始森林和丰富的野生动植物资源，其中最著名的是其壮观的冰川景观。海螺沟一共有三条沟，分别为一号沟、二号沟和三号沟。一号沟被称为“长虹卧雪”，是一条长约6公里的峡谷，两侧山峰高耸入云；二号沟被称为“犀牛望月”，是一片开阔的草甸，中间有一条小溪流过；三号沟被称为“一线天”，是一条狭窄的山谷，两旁峭壁陡峻，只有一条狭缝可供人通过。整个海螺沟景区以冰川为主体，辅以雪山、温泉、溶洞、彩池等多种自然景观，是一个集观光、休闲、探险于一体的旅游胜地。

离开海螺沟景区后，我们继续赶路，大约下午六点左右到达新都桥。新都桥位于四川省甘孜藏族自治州西北部，距离海螺沟景区约120公里。新都桥素有“摄影家的天堂”之称，因其独特的地形地貌和美丽的自然风光而闻名于世。新都桥是一座美丽的小镇，街道两旁绿树成荫，鲜花盛开，房屋错落有致，充满了浓郁的藏族风情。在这里，你可以漫步在石板路上，感受小镇的宁静与祥和；也可以骑上一匹骏马，驰骋在草原上，感受大自然的鬼斧神工；还可以坐在客栈里，品一杯香浓的酥油茶，静静地欣赏窗外的美景。总之，新都桥是一个让人流连忘返的地方。



### Day 3: 新都桥 - 雅江 - 理塘 - 稻城亚丁

第三天上午，我们从新都桥出发，前往稻城亚丁。稻城亚丁位于四川省甘孜藏族自治州南部，距离新都桥约300公里。稻城亚丁是国家AAAAA级风景区，也被誉为“最后的香格里拉”。稻城亚丁主要由三大景区组成，分别为洛绒牛场、夏诺多吉神山和央迈勇神山。这三个景区各具特色，相互辉映，共同构成了稻城亚丁的全貌。洛绒牛场被誉为中国最美的牧场之一，这里有高山草甸、蓝天白云、牦牛羊群和淳朴的牧民，构成了一幅和谐的画面。夏诺多吉神山巍峨挺拔，气势磅礴，山顶终年积雪，白雪皑皑，给人一种神圣的感觉。央迈勇神山则是稻城亚丁的最高峰，海拔高度为5958米，站在山顶上，可以俯瞰整个稻城亚丁的风光。除此之外，稻城亚丁还拥有众多的珍稀动植物，如黑颈鹤、金丝猴、杜鹃花等，这些都是大自然赐予人类的宝贵财富。



离开稻城亚丁后，我们继续赶路，大约下午七点左右到达理塘。理塘位于四川省甘孜藏族自治州西部，距离稻城亚丁约100公里。理塘有着悠久的历史 and 深厚的文化底蕴，当地居民大多信奉藏传佛教，因此理塘又被称为“天空之城”。理塘最著名的景点当属格聂神山，格聂神山主峰高达6204米，周围环绕着十座山峰，形态各异，蔚为壮观。除了格聂神山外，理塘还有许多其他值得一去的景点，如毛垭大草原、兔儿山、卡子拉山等。这些景点各有特色，相得益彰，共同构成了理塘的多姿多彩。


离开理塘后，我们继续赶路，大约傍晚时分到达稻城县。稻城县位于四川省甘孜藏族自治州北部，距离理塘约150公里。稻城县历史悠久，文化底蕴深厚，自古以来就是重要的交通枢纽和贸易中心。稻城县的名胜古迹众多，主要有丹巴碉楼、甲居藏寨、色达喇荣五明佛学院等。此外，稻城县的自然风光也十分优美，主要景点有然乌湖、波密桃花沟、鲁朗林海等。在这些景点的衬托下，稻城县显得更加生机勃勃，令人流连忘返。




## 三、总结

总的来说，这次稻城亚丁之行是一次难忘的经历。虽然一路上遇到了很多困难和挑战，但我们一家人齐心协力，克服了困难。


Figure A13. Interleaved composition generated by InternLM-XComposer.

 🤔


Describe this image?

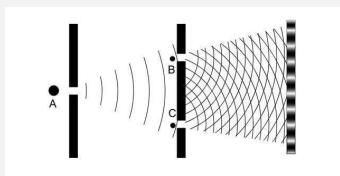
 The image depicts a young man and a young woman dressed in school uniforms walking down a staircase in a city setting. They appear to be enjoying their time together, with the man leading the way.

Which movie does this image come from? 🤔


 This image comes from the anime movie "Your Name."

Describe the story of this movie. 🤔


 "Your Name" is a 2016 Japanese animated romantic fantasy film directed by Makoto Shinkai. The movie follows the story of a high school boy named Taki and a high school girl named Mitsuha, who find themselves mysteriously connected to each other in their dreams.


 🤔

Describe this image.


 The image depicts a diagram of a wave passing through a double slit experiment. There are two slits, A and B, and a single particle, represented by a black dot, is passing through one of them. The wave pattern created by the particle is shown on the left side of the diagram, while the double slit is located on the right side.

Who discovered it? 🤔


 The double slit experiment was discovered by Thomas Young in 1801.


 🤔

What is the funny thing in this image?


 The funny thing in this image is that a car has been covered in snow, giving it the appearance of having a face. Specifically, the car has a nose, eyes, and a mouth, making it look like a snowman. This is a creative and humorous way of transforming a car into a snowman, adding a touch of whimsy to the scene.

What is the snowman's mood? 🤔

 The snowman's mood appears to be happy or playful, as it has a smile on its face.

 🤔

Describe this image in detail.

 The image depicts a cartoonish depiction of a man's finger with a gun drawn on it. The gun is pointed directly at the man's face, creating a tense and threatening atmosphere. The man's face is also drawn on the finger, with a sad expression on his face.

Will the finger get hurt? 🤔


 No, the finger will not get hurt.

Figure A14. Chat with InternLM-XComposer.



能简单介绍一下这张图上的内容吗？



这幅油画描绘了一辆红色老爷车停在一座城市街道上，车旁有一棵高大的枫树。整幅画面呈现出一种宁静的氛围，似乎在讲述一段温馨的回憶。

从美学的角度分析下这幅油画，聊一聊其颜色搭配、构图、光影上的特点。



这幅油画在颜色搭配上非常和谐，红色老爷车和枫树的颜色相得益彰，整个画面呈现出一种温馨、怀旧的氛围。构图上，老爷车占据了画面的主要部分，而枫树则作为背景，衬托出老爷车的风采。在光影方面，这幅油画运用了柔和的光线，使得整幅画面呈现出一种宁静、温馨的氛围。老爷车和枫树在阳光的照射下，显得更加迷人。

这种老爷车在什么时候比较流行？



这种老爷车在20世纪30年代至40年代非常流行，当时被称为“老爷车”或“老式车”。这种车型的特点是车身修长、线条流畅，通常采用V8发动机，动力强劲，适合长途驾驶。它们在当时的美国、欧洲和澳大利亚等地非常受欢迎，成为了那个时代的一种标志性



请你描述一下这张图片



图片描绘了一个蓝色背景，上面有一只卡通时钟，钟面上显示着数字。时钟周围有一些星星和云朵，给整个画面增添了梦幻的氛围。



这张图片描绘了一个卡通女孩，她的头发是蓝色的，眼睛周围有星星和云朵，看起来非常梦幻。她的面部表情似乎有些悲伤，可能正在哭泣。



两张图片之间有相似之处吗？比如风格、背景上

两张图片在风格和背景上都有相似之处，都采用了卡通、梦幻的风格，背景都有星星和云朵的元素。



图中是什么？



麻将桌和麻将



图中的麻将牌们构成了什么番型？

图中的麻将牌们构成了“九莲宝灯”的番型



接下来，我抓到一张么鸡，请问我能胡牌吗？

是的，你抓到一张么鸡，可以胡牌。

Figure A15. Chat with InternLM-XComposer.